

Assessment of RCA4, CORDEX Africa domains RCMs Performance in Simulating Rainfall and Temperature: A case of Gilgal Gibe watershed, Ethiopia

Authors: Keder Hussen Farah, * ^{1,2} Chala Hailu Sime³ Usame Mohamed Muhumed⁴ Abdifatah Mohamed Hassen⁵

Affiliations:

¹ Jimma University, School of Civil and Environmental Engineering

² Somali Regional State Irrigation development Buruea

³ Jimma University, School of Civil and Environmental Engineering.

⁴ Jigjiga University, Department of Hydraulic and Water Resource Engineering. U

⁵ Jimma University, School of Civil and Environmental Engineering.

Corresponding Author:
Khadarhiral@gmail.com*

ABSTRACT

Examining the spatiotemporal dynamics of meteorological variables in the context of changing climate, particularly in countries where rainfed agriculture, and hydropower project are predominant, is vital to assess climate-induced change. CORDEX Africa has been developed to forecast Africa's climate variation and variabilities. the RCA4 regional climate model performance of CORDEX Africa domains have not been evaluated yet. Therefore, this finding is aimed to evaluate RCA4 CORDEX Africa RCMs performance in the Gilgal Gibe Watershed, Omo basin, Ethiopia. The observed rainfall and temperature data for five stations obtained from National Metrological Agent were used for bias correction of the RCMs. First the accuracy of simulation results was evaluated using as suite of statistical measures such as Bias, Root Mean Squared Error (RMSE) and correlation coefficient, and the result was found that the performance of model is satisfactory. After evaluating performance model, the data have been analyzed using coefficient of variation, anomaly index and precipitation concentration index. Furthermore, Mann-Kendell test was used to detect the time series trend. the result revealed that there is non-significantly declining of trend for annual in all stations: -0.0101cm/year , $:0.0044\text{cm/year}$: -0.00441cm/year , 0.0057cm/year , and -0.0939cm/year for Dedo, Assendabo, Sekoru, Omonad and Jimma, respectively. and for maximum and minimum temperature the result has shown that there is significant increasing trend in annually. lastly future climate change (2025-2050) have been investigated, and 60% of stations have shown decrease in annual rainfall under RCP4.5, and RCP8.5 scenario. where temperature of study area has shown that there is increasing monthly maximum and minimum temperature in all stations under RCP4.5, and RCP8.5 scenario.

Key Words: Climate Change, Gilgel Gibe Watershed, Ethiopia, MK test, RCP, RCM and Trend Analysis

INTRODUCTION

Impacts of climate variability and change are increasingly becoming a challenge in tackling food and water security problems worldwide. There is immense public concern on unpredictable or extreme weather and climate induced events and keen interest is on the coming decades' dynamic behavior of such events. Understanding climatic historical changes is necessary for optimization of water resources and food production. Historical datasets are important means of obtaining information on the temporal patterns of rainfall and temperature time series for climatological and hydrological applications such as hydrological modeling, climate variability, water resources planning and management for various uses including agricultural production, environmental flows and engineering designs (Langat et al., 2017). The seasonal and inter-annual spatial and temporal variability of rainfall and temperature in a changing climate scenario is vital for water resource availability, management, and utilization within a river basin (Mahajan & Dodamani, 2015).

Precipitation and temperature are two of the most important variables in the field of climate sciences and hydrology frequently used to trace extent and magnitude of climate change and variability. Precipitation is a vital part of the hydrologic cycle and changes in its pattern would directly influence the water resources of the concerned region. Changes in rainfall quantity and frequency would alter the pattern of stream flows and demands, spatial and temporal distribution of runoff, soil moisture, and groundwater reserves. This will necessitate a review of reservoir operation and water resources management policies (Asfaw et al., 2018).

Temperature is also considered a good indication of the state of climate because of its ability to represent the energy exchange process over the earth's surface with reasonable accuracy (Jain et al., 2013). The temporal variability analysis of rainfall and temperature at timescales help in determining the likelihood of extreme (drought or flood) event occurrences and management of water resources particularly for major consuming sectors; namely agriculture, hydropower and domestic water supply within basins (Langat et al., 2017).

Study of different time series data have proved that trend is either decreasing or increasing, both in case of temperature and rainfall. (Mondal et al., 2012) investigated in

rainfall trend analysis by Mann-Kendall test in North-Eastern part of Cuttack District, Orissa observed that there is evidence of some change in the trend of precipitation of the region in these 40 years in different month. In Kenya, (Langat et al., 2017) studied temporal variability and trends of rainfall and streamflow in Tana River basin and reported Annual rainfall trend analysis showed negative monotonic trend in seven rainfall stations and positive trends in three stations, indicating an increasing rainfall in high elevation areas, and more drying conditions for low areas within the basin. A study by (Asfaw et al., 2018) in Northcentral of Ethiopia pointed out that there is declining trend for annual and kiremt rainfall was found to be statistically significant while that of belg was not significant. Therefore, in-depth knowledge and analysis of rainfall and temperature regimes on different time scales are increasingly becoming necessary for enhancing the management of water resources, planning and designing of hydraulic structures, agriculture production and to mitigate the negative effects of floods and droughts.

In East and Southern African regions, seasonal variations in rainfall as well as the rate of evapotranspiration describe the periodic weather patterns. Aberrant rainfall variability affects major water resources and reservoirs, wetlands, agriculture and socio-economics of rural farmers whose livelihoods are significantly derived from rain-fed systems of production (Langat et al., 2017). In terms of rainfall occurrence, there are three seasons in Ethiopia, namely bega (dry season) which extends from October–January, belg (short rainy season) which extends from February–May and kiremt or meher (long rainy season) which lasts from June–September (Tadege 2007). Rainfall in the short rainy season (belg) is caused by moist easterly and south-easterly winds from the Indian Ocean, while in the main rainy season (kiremt) is a result of convergence in low-pressure systems and the Intertropical Convergence Zone (Aden 2015).

Sea surface temperature changes and El-Nino Southern Oscillation (ENSO) episodes in the Atlantic and Indian~ Oceans do have remarkable implication in the timing and amount of rainfall in Ethiopia particularly underscored that, drought events in Ethiopia are caused by ENSO along with sea surface temperature (SST) anomalies in the Southern Atlantic and Indian Oceans combined which is exacerbated with anthropogenic activities. Rainfall distribution in Ethiopia affected by ENSO events and SST anomalies by displacing and weakening the rain-producing air masses. Kiremt rain account for 50–80% of annual rainfall totals in Ethiopia, which has high contribution to agricultural productivity and major water reservoirs (Dereje Ayalew, 2012; Wagesho et al., 2013).

Variations of the temperature have also impacted the agricultural crop yield. Hence, the main objective of this study is Assessment of RCA4, CORDEX Africa domains RCMs Performance in Simulating Rainfall and Temperature which intern help use to analysis further impact of climate change on water resources and agricultural crop yield.

Trend analysis conducted so far in Ethiopia are not conclusive and some are conducted at macro scale; which needs further study. In Gibe River is an important river that maintain mega hydropower projects (Gibe I and Gibe II), which plays a significant role for the sustainable economic growth of Ethiopia (Jillo et al., 2017). On the other hand, Gibe River and Omo-gibe River discharge is highly dependent on the flow generated from upper Gibe basin, any problems which alters the discharge levels in the upper Gibe basin may have considerable effect on the total flow of Gibe and Omo-gibe River and consequently effect the agricultural activities in south/southeast and hydropower projects. Therefore, analyzing, characterizing, and understanding of rainfall and temperature variability and trends under both RCP4.5 and RCP8.5 scenarios is useful for water resources planning and development in this study area.

MATERIALS AND METHODS

Description of the Study Area

The Gilgel Gibe basin is one of the major river basins in Ethiopia and is situated in the south western part of the country covering parts of South/southeast. The confluence of the large Gibe River 4.00° and $8^{\circ}19'N37^{\circ}28'E/8.31^{\circ}N37.467^{\circ}E$ with smaller Wabe river forms the larger Omo River. The basin is largely comprised of cultivated land. In general terms, the Gilgel Gibe basin is characterized by high relief hills and mountains with an average elevation of 1700m above the sea level.

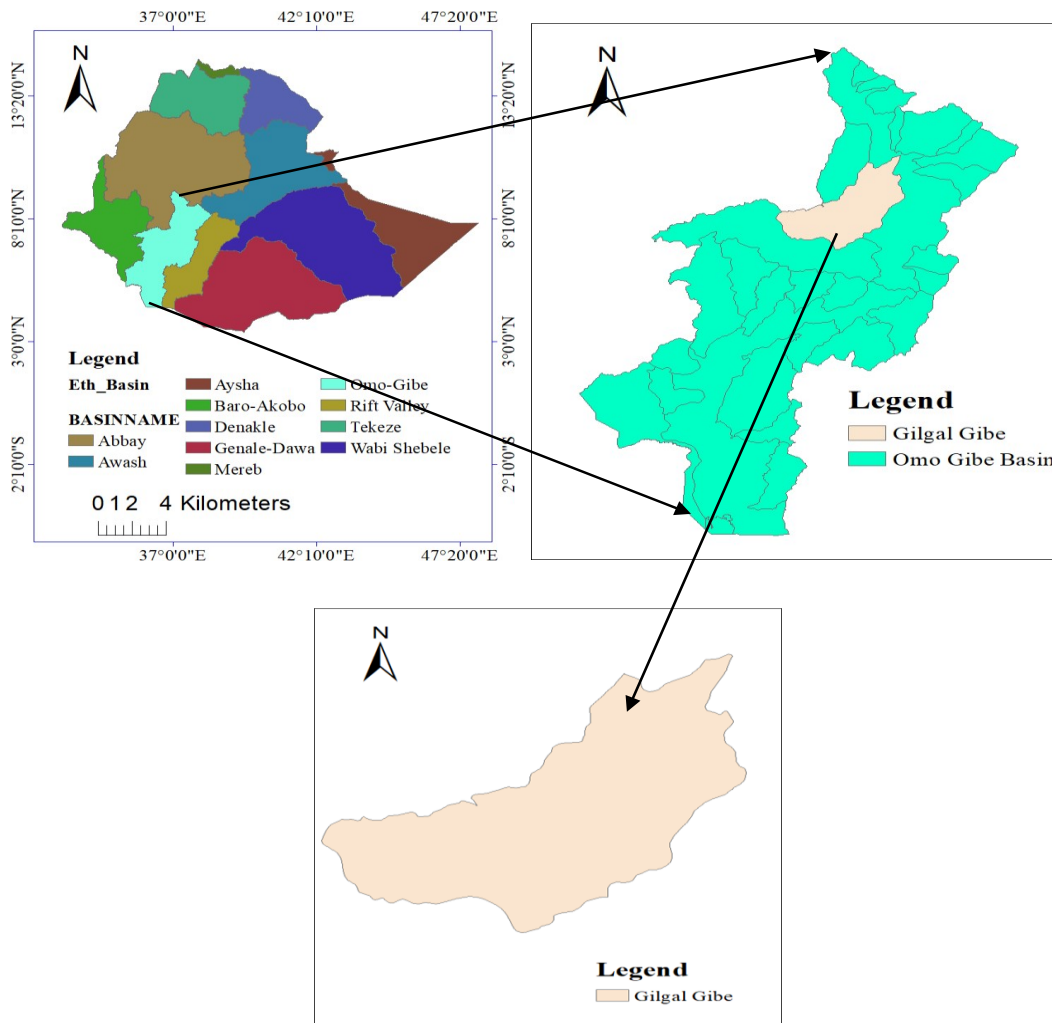


Figure 3. 1 Study Area

Data Collection and Analysis

The data used for this study are: Daily Maximum and minimum temperature, rainfall data, Digital Elevation Model and RCM data. All observed weather data used in the study were collected from the national meteorology service of Ethiopia (NMA). The dataset covers the reference period of 1987-2017.

Daily rainfall and temperature RCA4, RCM simulated from the CORDEX Africa domain derived by ICHEC-EC-EARTH was selected and downloaded. RCA4 is served by GCM of Sveriges Meteorologiska och Hydrologiska Institute (SMHI), Sweden. It is called as SMHI_RCA4 or simply as RCA4. The data from RCA4 are served by two illustrative concentration pathways (RCP) i.e. mid-range mitigation (RCP4.5) emission scenarios and high emission (RCP8.5) scenario. Rainfall and temperature data were extracted from downloaded data in ArcGIS.

Spatial Data

Digital Elevation Model (DEM) is any digital representation of a topographic surface and specifically to a raster or regular grid of spot heights. It is the basic input of GIS hydrologic model to delineate watersheds and River networks. The first step in creating the model input is the watershed delineation accomplished using digital elevation data. In this study, DEM will use to analyze the spatial distribution of the average rainfall and temperature. DEM will be collected from MoWIE.

Tools used

Data analysis was undertaken using R software, and excel spreadsheet. Various software such as GIS, XLSTAT2018. RStudio will be used to analysis the data; GIS will be used to analysis the spatial distribution of the rainfall and temperature; XLSTAT2018, to fill the missing data; Excel will be used to arrange data.

Method used

In this investigation, the variability of rainfall and temperature were analyzed. Rainfall is a key component of the hydrological cycle and temperature is also considered a good indication of the state of climate because of its ability to represent the energy exchange process over the earth's surface with reasonable accuracy. The data used in this research are DEM data, Meteorological data, and RCM data.

First, the raw rainfall, maximum and minimum temperature daily records were examined and checked for missing values. The data were examined using Excel and missing data were filled using XLstat2018, then the data were considered appropriate for analysis and R programming language for data analysis was used in preprocessing (cleaning) the data, analysis and visualization. Secondly, the daily and monthly precipitation and temperature time series were aggregated annually and also in monthly trimesters as December–January–February (winter), March–April–May (spring), June–July–August (summer) and September–October–November (autumn) seasons, with the aim of observing potential changes at the seasonal scale and identifying outstanding monotonic trends. Finally, the trend analysis was performed using time series plots and Mann–Kendall test. The method of analysis was RStudio (2014 version) which is an integrated development environment (IDE) for the R programming language. The `precintcon` package in RStudio was used to analyze the precipitation intensity, concentration and anomaly because of its capability functions in the management, analysis, and plotting of time series (month, annual and seasonal) from daily and monthly data.

Furthermore, for assessing of future climate projection in the selected sub-basin the following three major steps has been followed first.

First, the outputs of the simulation starting from (1985-2050) were ensemble and analyzed. The period was separated into two-time slices namely Historical (1985- 2017), and future (2025-2050). The study determines the future rainfall and temperature variability.

Second, the daily RCMs output are extracted from grid cells covering the Gilgel Gibe basin from the available source and the performance of the dynamically downscaled models' simulations were evaluated. Bias corrections were carried out for RCMs output to the nearby observed stations on

the watershed; then the future changes in maximum and minimum temperature and precipitation were assessed in the basin.

Third, the bias corrected RCM outputs is used in R programming language in order to understand the variability and significant behavior of the rainfall and temperature for the scenario periods in the Gilgel Gibe watershed. The bias correction of climate outputs was using power transformation for precipitations and Variance scaling method for temperature, by comparing the observed precipitation and temperature at each station with the overlapping grid points of the RCM.

Model Performance

The pairwise comparison statistics techniques such as Pearson correlation coefficient (r), Mean Error (ME), Root Mean Square Error (RMSE) and Bias were used to evaluate the performance of satellite estimates of rainfall and temperature. Those comparison techniques were used to check performance and agreement between the observed and simulated meteorological data. (Nile and Bayissa, 2017; Tamiru and Rientjes, 2015)

The Pearson correlation coefficient (r) is used to measure the goodness of fit and linear association between two variables. It measures how well the satellite rainfall and temperature product corresponds to the observed rainfall and temperature. Its value ranges between 0 to 1 in which one indicates the perfect score.

$$r = \frac{\sum(O - \hat{O})(S - \hat{S})}{\sqrt{\sum(O - \hat{O})^2} \sqrt{\sum(S - \hat{S})^2}} \dots\dots\dots(2.1)$$

where r is the correlation coefficient, O = gauge rainfall or temperature measurement, \hat{O} = average gauge rainfall or temperature measurement, S = satellite rainfall or temperature simulate, \hat{S} = average satellite rainfall or temperature simulate, and n = number of data pairs.

The RMSE is used to measure the average magnitude of the estimated errors between the satellite(simulated) and the observed rainfall and temperature; A lower RMSE value means greater central tendencies and small extreme error. RMSE value of zero is the perfect score.

$$RMSE = \sqrt{\frac{1}{n} \sum(S - O)^2} \dots\dots\dots(2.2)$$

where RMSE is the root mean square error, O = gauge rainfall and temperature measurement, and S = satellite rainfall and temperature estimate.

Bias reflects how well the mean of the satellite rainfall and temperature corresponds with the mean of the observed rainfall and temperature; A Bias value closer to one indicates the cumulative satellite data estimate is closer to the cumulative observed data. Bias value of one is the perfect score.

$$\text{Bais} = \frac{\sum S}{\sum O} \dots\dots\dots(2.3)$$

where O = gauge rainfall or temperature measurement, and S = satellite rainfall or temperature estimate.

Coefficient of Variation (CV)

Variability analysis involves the use of Coefficient of Variation (CV). CV was used to evaluate the variability of the rainfall. A higher value of CV is the indicator of larger variability, and vice versa which was computed as:

$$\text{CV} = \frac{\sigma}{\mu} \times 100 \dots\dots\dots 2.4$$

Where CV is the coefficient of variation; σ is standard deviation and μ is the mean precipitation. According to Hare (2003), CV will be used to classify the degree of variability of rainfall events as less (CV < 20), moderate (20 < CV < 30), and high (CV > 30).

Precipitation Concentration Index (PCI)

PCI was used to examine the variability (heterogeneity pattern) of rainfall at different scales (annual or seasonal). The PCI values was computed, as given by Oliver (1980) (Abdullah et al. 2010) as:

$$\text{PCI}_{\text{annual}} = \frac{\sum_{i=1}^{12} P_i^2}{(\sum_{i=1}^{12} P_i)^2} \times 10 \dots\dots\dots 2.5$$

where: P_i = the rainfall amount of the i th month.

According to Oliver (1980), PCI values of less than 10 indicates uniform monthly distribution of rainfall (low precipitation concentration), values between 11 and 15 denote moderate

concentration, values from 16 to 20 indicates high concentration, and values of 21 and above indicate very high concentration.

Standardized anomalies

Standardized anomalies of rainfall were calculated to examine the nature of the trends, enables the determination of the dry and wet years in the record and used to assess frequency and severity of droughts ((Asfaw et al. 2018) as:

$$Z = \frac{(X_i - \bar{X})}{s} \dots\dots\dots 2.6$$

where: Z is standardized rainfall anomaly; X_i is the annual rainfall of a particular year; \bar{X} is long term mean annual rainfall over a period of observation and ‘s’ is the standard deviation of annual rainfall over the period of observation.

Rainfall and Temperature and trend analysis

Trend detection and analysis are performed through parametric and non-parametric tests only for consistent data. Normality and homogeneity of variance throughout the series may be adversely affected by outliers and missing data in parametric tests. The advantage of non-parametric statistical test over the parametric test is that the former is more suitable for nonnormally distributed, outlier, censored and missing data, which are frequently encountered in hydrological time series. As a result, Mann Kendall (MK) test is widely used to detect trends of meteorological variables (Asfaw et al., 2018). MK test is a nonparametric test, which tests for a trend in a time series without specifying whether the trend is linear or non-linear (Taxak et al., 2014).

MK trend test is a non-parametric test commonly employed to detect monotonic trends in series of environmental data, climate data or hydrological data. MK test has been used to detect the presence of monotonic (increasing or decreasing) trends in the study area and whether the trend is statistically significant or not. Since there are chances of outliers to be present in the dataset, the non-parametric MK test is useful because its statistic is based on the (+ or -) signs, rather than the values of the random variable, and therefore, the trends determined are less affected by the outliers (Birsan et al., 2005). The MK test statistic ‘S’ was calculated based on Mann (1945), Kendall (1975) and Yue et al. (2002) using the formula:

$$S = \sum_{i=1}^{n-1} \sum_{j=i+1}^n \text{sgn}(x_j - x_i) \quad (2.7)$$

The application of trend test was done to a time series X_i that is ranked from $i = 1, 2 \dots n-1$ and X_j , which is ranked from $j = i+1, 2 \dots n$. Each of the data point X_i is taken as a reference point which is compared with the rest of the data point's X_j so that:

$$\text{sgn}(X_j - X_i) = \begin{cases} +1 & \text{if } (X_j - X_i) > 0 \\ 0 & \text{if } (X_j - X_i) = 0 \\ -1 & \text{if } (X_j - X_i) < 0 \end{cases} \quad (2.8)$$

where: X_i and X_j are the annual values in years i and j ($j > i$) respectively.

It has been documented that when the number of observations is more than 10 ($n \geq 10$), the statistic 'S' is approximately normally distributed with the mean and $E(S)$ becomes 0 (Kendall, 1975). In this case, the variance statistic is given as:

$$\text{Var}(S) = \frac{n(n-1)(2n+5) - \sum_{t=1}^n t_1(t_1-1)(2t_1+5)}{18} \quad (2.9)$$

where: n is the number of observation and t_i are the ties of the sample time series. The test statistics Z_c is as follows:

$$Z = \begin{cases} \frac{S-1}{\sigma} & \text{if } S > 0 \\ 0 & \text{if } S = 0 \\ \frac{S+1}{\sigma} & \text{if } S < 0 \end{cases} \dots\dots\dots 2.10$$

where Z_c follows a normal distribution, a positive Z_c and a negative Z_c depict an upward and downwards trend for the period respectively. Sen's Slope estimation test computes both the slope (i.e. the linear rate of change) and intercept according to Sen's method. The magnitude of the trend is predicted by Theil (1950) and Sen (1968) slope estimator methods. A positive value of β indicates an 'upward trend' (increasing values with time), while a negative value of β indicates a 'downward trend'.

Here, the slope (T_i) of all data pairs is computed as (Sen, 1968). In general, the slope T_i between any two values of a time series x can be estimated from:

$$T = \frac{x_j - x_i}{j - i} \quad (2.11)$$

where: x_j and x_k are considered as data values at time j and k ($j > i$) correspondingly. The median of these N values of T_i is represented as Sen's estimator of slope which is computed as $Q_{med} = T_{(N+1)/2}$ if N appears odd, and it is considered as $Q_{med} = [T_{N/2} + T_{((N+2)/2)}/2]$ if N appears even. A positive value of Q_i indicates an upward or increasing trend and a negative value of Q_i gives a downward or decreasing trend in the time series.

Regional Climate Model Data

The climate model data used were obtained from outputs of high-resolution regional climate models of CORDEX RCMs (Fekadu et al. 2019) dynamically downscaled by the regional climate model of consortium for small scale modeling, Climate Limited area Modeling (COSMO-CLM or CCLM, <http://www.clm-community.eu>). The COSMO-CLM model uses large scale lateral boundary conditions from four GCMs; CNRM, MPI_ESM_LR, EC_EARTH and HadGEM2ES. An ensemble of the CCLM model has historical runs driven by 4 different GCMs, which covers from 1950-2005 for control period whereas the projections (2006-2100) are forced by two representative concentration pathways (RCPs), namely RCP4.5 and RCP8.5 future emission scenarios. The future climate change scenarios considered for this investigation consisted of three GCMs (CNRM, MPI_ESM_LR (MPI) and EC_EARTH) due to time limitation. These future climate emission scenarios are based on the fifth Intergovernmental Panel for climate change (IPCC) report (Endris et al., 2013). The data correspond to two RCP scenarios of RCP4.5 and RCP8.5 for the period 1950-2100 can be obtained from CORDEX-Africa database. The selected two RCPs are medium-low and high radiative forcing scenarios, respectively. The two RCPs use radiative forcing values of 4.5 and 8.5 W/m^2 , respectively.

1. The first step was to download simulated daily maximum and minimum temperatures and daily amounts of precipitation from CORDEX project (Coordinated Regional Climate Downscaling Experiment) at spatial grid resolution of 0.44o (~50 Km) (<http://esgfdata.dkrz.de/login/?next=http://esgf-data.dkrz.de/search/cordex-dkrz/>)
2. The second step was to extract the RCM overlapping grids that fall into the study area for the Selected gauging stations from step one. Then, basin average climate model time series data were calculated using area weighted average for ten grid boxes.
3. The third and final step was to calculate the biases for the historical and future scenarios. In this step the bias correction is for daily precipitation and temperature data. Figure 4.5 shows location of all grid points within the catchment.

Correction of Biased RCM simulations

Purpose of Bias Correction

Bias correction procedures employ a transformation algorithm for adjusting RCM output. The underlying idea is the identification of possible biases between observed and simulated climate variables, which is the basis for correcting both control and scenario RCM runs. Bias correction methods are assumed to be stationary, i.e., the correction algorithm and its parameterization for current climate conditions are also valid for future conditions. The following bias correction methods to adjust RCM simulations were used: (1) power transformation, (2) variance scaling.

Power Transformation for Precipitation

The precipitation is usually varied spatially and highly nonlinear in nature. Power transformation is a nonlinear method which corrects both mean and variance of precipitation (Yang, et al, 2015). In this study the RCM data of precipitation was bias corrected by using Power Transformation Method because it corrects the mean, variance and coefficient of variation (CV), leads to a better copy of observed precipitation. The correction method is applied by comparing the daily observed precipitation at each station with the nearest grid point of the RCM considering the grid points as a single station on the watershed. The power transformation method is explained in the following equations:

$$P^* = (a \cdot P^b) \dots\dots\dots 2.12$$

Where, P* is corrected precipitation, P is simulated precipitation. The parameters a and b is

estimated by equalizing the coefficient of variation (CV) of the corrected simulations P_b and CV of the observed values, both from the calibration/optimization period. Parameter b was first determined iteratively by ensuring that the CV of the corrected precipitation matched that of the observed. Then parameter a , which depends on the value of b , was determined by matching the means of the corrected and observed precipitation.

Variance Scaling for Temperature

The PT method is an effective method to correct both the mean and variance of precipitation, but it cannot be used to correct temperature time series, as temperature is known to be approximately normally distributed (Yang et al, 2015). The VARI method was developed to correct both the mean and variance of normally distributed variables such as temperature (Teutschbein and Seibert 2012). Temperature is normally corrected using the VARI method.

$$T_{corr} = T_{obs} + \frac{\sigma(T_{obs})}{\sigma(T_{rcm})} (T_{rcm} - \overline{T_{rcm}}) \dots\dots\dots 2.13$$

Where: T_{corr} the corrected daily temperature: T_{rcm} the uncorrected daily temperature from RCM model and T_{obs} the observed daily temperature while obs is mean observed temperature and $\overline{T_{rcm}}$ is mean simulated temperature.

Results and Discussions

Model Performance

The calibration is carried out for thirty-five year, 35yrs, period from January 1st, 1985 to December 31st, 2017. We first compared basin mean annual rainfall, maximum and minimum temperature amount of Gilgel Gibe as obtained from gauged data and model. The daily bias corrections between the observed and simulated variables during the control period for each RCM models were applied. The bias correction was done on RCM-simulated precipitation, max/min temperature, the PT and VARI methods were used for the five extracted nearby stations.

Rainfall model performance

Table 4.1, figure 4.6 and figure 4.7 shows the statistical indicators obtained for weather stations against the different satellite estimates. In general, the result shows a good agreement between the weather stations and satellite estimates. The smallest bias of 2.650% is shown for Jimma Station which suggests that basin wide rainfall is quite well captured and represented. This shows there is a good agreement between the cumulative values of Dedo, and Omonad with bias of 2.954, and 3.543. Assendabo showed high mean Bias (8.257, and 9.1496 under RCP4.5 and RCP8.5) and hence the cumulative values were underestimated satisfactorily. The cumulative rainfall values of all stations were underestimated in all stations except Sekoru (Bias=10.416, and 11.266 under RCP4.5 and RCP8.5) which is overestimated. In general, biases of most of the models can be considered relatively large with values larger than + or -10%. Values as such indicate a need to correct the systematic error of RCM outputs before receiving application by users. For RMSE performance measure, Sekoru has the smallest value (112.4, and 119.3 mm per year under RCP4.5, and RCP8.5 respectively) whereas Dedo resulted in the largest value (162.4, 166.4mm per year under RCP4.5, and RCP8.5 respectively).

In terms of bias, and RMSE, all stations were performed satisfactorily except Sekoru which performed poorest. However, this is not indicated when the correlation coefficient is used as an assessment criterion. There is a weak correlation (i.e. linear relationship) between the annual rainfall amount from most models and the reference data. The correlation coefficient is between than 0 to 1 for none of the stations except Omonad performing best as the correlation coefficient is 0.041. However, we note that correlation coefficient values in general cannot be

considered high and thus suggest that outputs of none of the models well matched in-situ observations at annual base.

Figure 4.2 shows the scatter plots produced between the point-based Jimma data of the observed stations versus rainfall simulated. A relatively lower coefficient of determination values ($R^2 = 0.031$) was observed for Jimma rainfall estimates. The trend line of Jimma rainfall is converging to the 45° line, which shows the existence of a good agreement between Jimma observed and simulated rainfall.

Table 4. 1 Performance of the CORDEX-RCM simulations in capturing and representing mean annual rainfall over the upper Gilgel Gibe basin over the period 1985–2017.

Scenario	Performance Statistic	Stations				
	Statistical analysis	Jimma	Ascendabo	Dedo	Omonad	Sekoru
RCP4.5	RMSE	1.444	1.246	1.624	1.322	1.124
	PBIA	2.650	8.257	2.954	3.543	10.416
	r	-0.175	-0.028	-0.116	0.041	-0.101
RCP8.5	RMSE	1.481	1.3594	1.661	1.404	1.193
	PBIA	3.810	9.1496	4.005	4.302	11.266
	r	-0.208	-0.238	-0.151	-0.085	-0.077

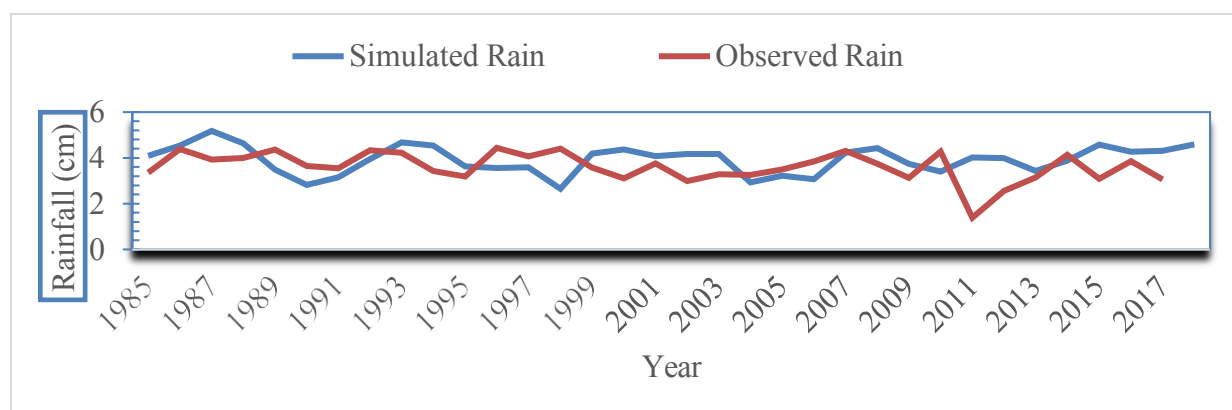


Figure 4. 1 Calibration result of average daily simulated and measured rainfall at the near Jimma, where Jimma gauging station is located by 4.5 model.

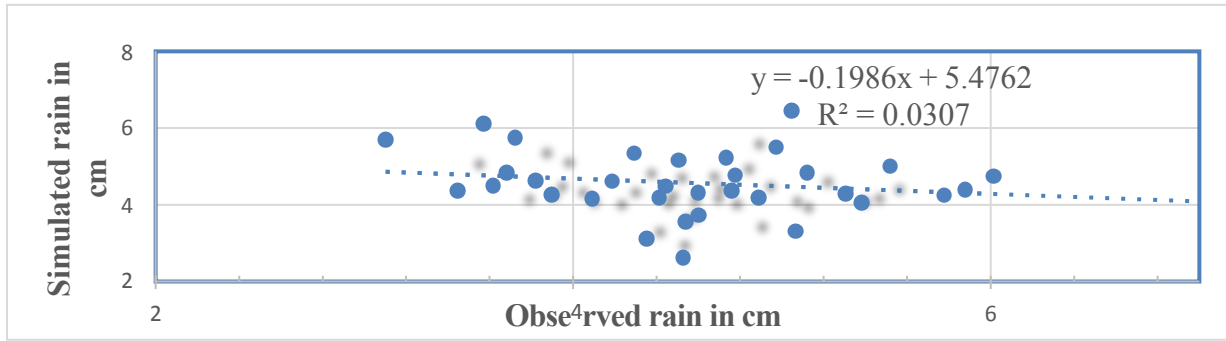


Figure 4. 2 Values of R^2 for calibration period.

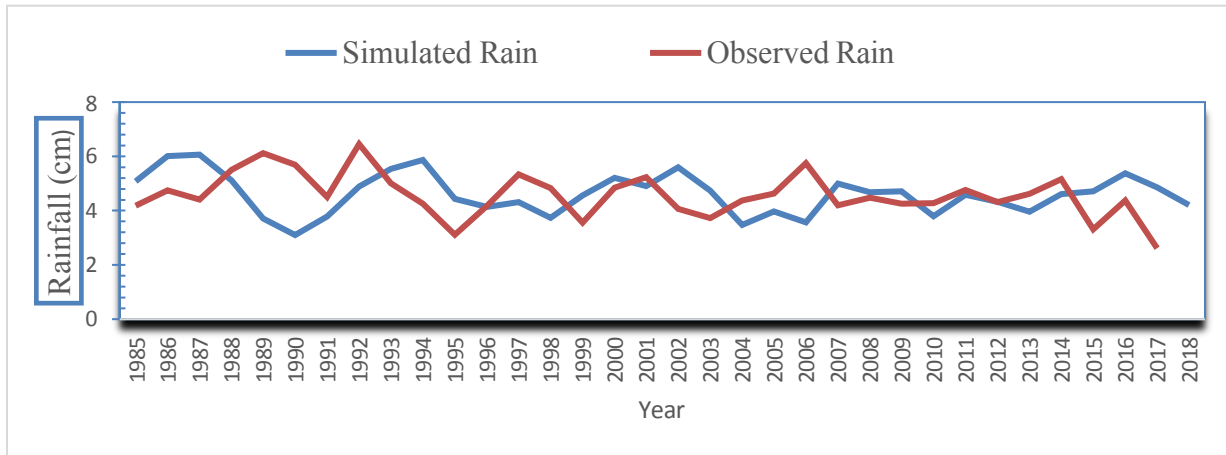


Figure 4. 3 Calibration result of average daily simulated and measured rainfall at the near Jimma, where Jimma gauging station is located by 8.5 model.

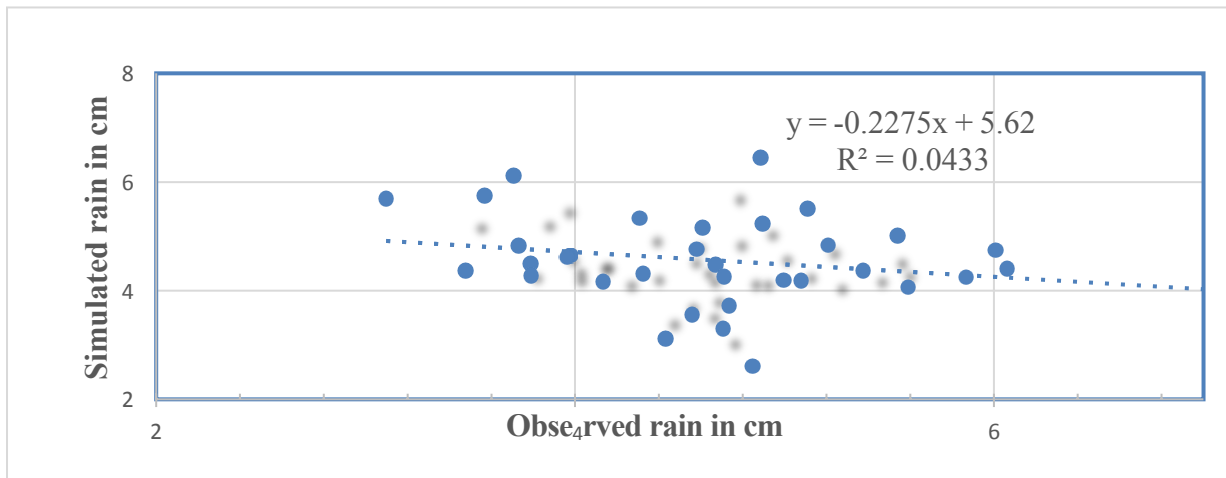


Figure 4. 4 Values of R^2 for calibration period 8.5.

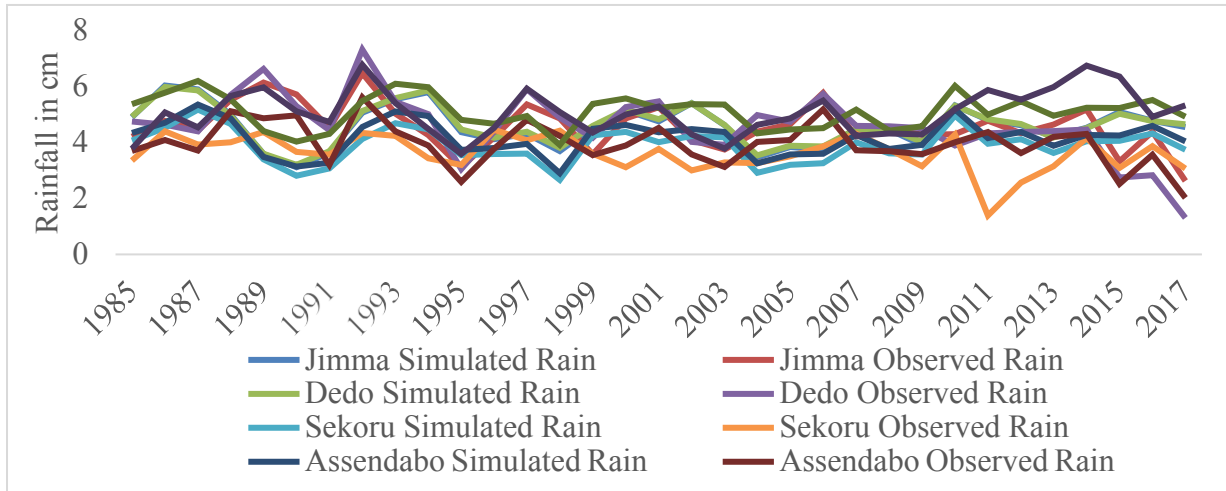


Figure 4. 5 Calibration result of average daily simulated and measured rainfall at all station by 4.5 model.

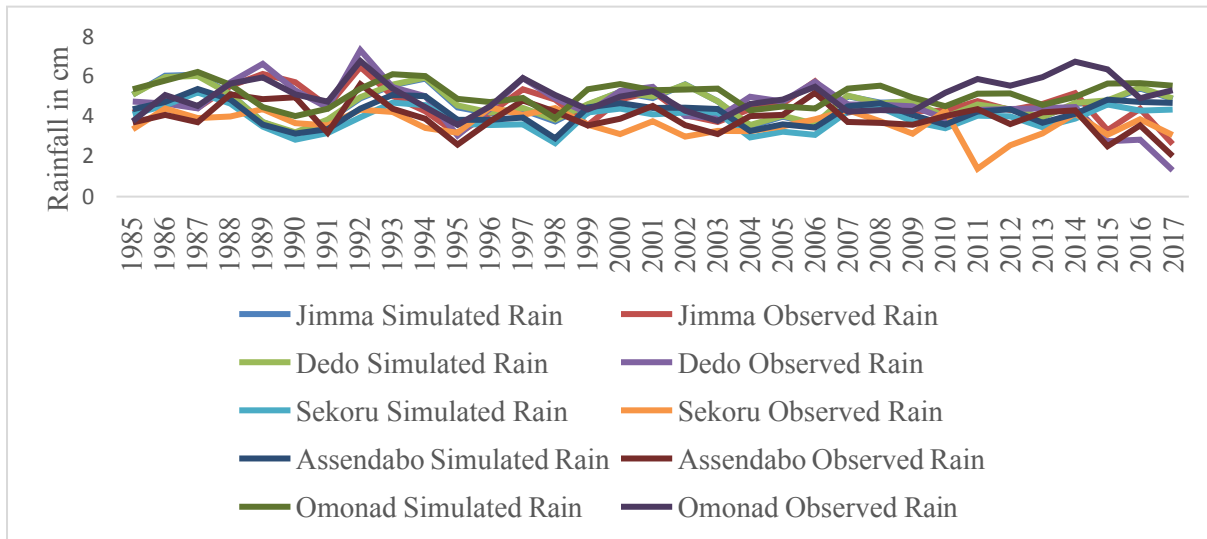


Figure 4. 6 Calibration result of average daily simulated and measured rainfall at all station by 8.5model.

Maximum Temperature Model Performance

Table 4.2, figure 4.9 and figure 4.11 shows the statistical indicators (maximum temperature) obtained for weather stations against the different satellite estimates. In general, the result shows a satisfactory agreement between the observed and simulated maximum temperature. In terms of bias all stations were performed satisfactorily. However, this is not indicated when RMSE and coefficient of correlation(r) is used as an assessment criterion There is a weak correlation (i.e. linear relationship) between the minimum amount from most models and the reference data, and the average magnitude of estimated error is quite larger in maximum observed and simulated temperature.

Figure 4.10 shows the scatter plots produced between the point-based Jimma data of the observed stations versus simulated maximum temperature. A relatively lower coefficient of determination values ($R^2 = 0.003$) was observed for Jimma Tmax estimates. The trend line of Jimma Tmax is converging to the 45° line, which shows the existence of a good agreement between Jimma observed and simulated maximum temperature.

Table 4. 2 Performance of the CORDEX-RCM simulations in capturing and representing mean annual maximum temperature over the upper Gilgel Gibe basin over the period 1985–2017.

Scenario Tmax	Performance Statistic	Stations				
	Statistical analysis	Jimma	Ascendabo	Dedo	Omonad	Sekoru
RCP4.5	RMSE	5.1957	5.3440	4.7683	5.503	4.9250
	PBIA	4.5429	9.9817	8.7708	6.828	2.3067
	r	-0.0551	-0.2741	-0.2097	-0.091	-0.0689
RCP8.5	RMSE	5.2889	5.4201	4.8443	5.591	4.9904
	PBIA	4.6585	10.0865	8.9150	6.926	2.4070
	r	-0.1836	-0.2961	-0.1507	-0.208	0.0052

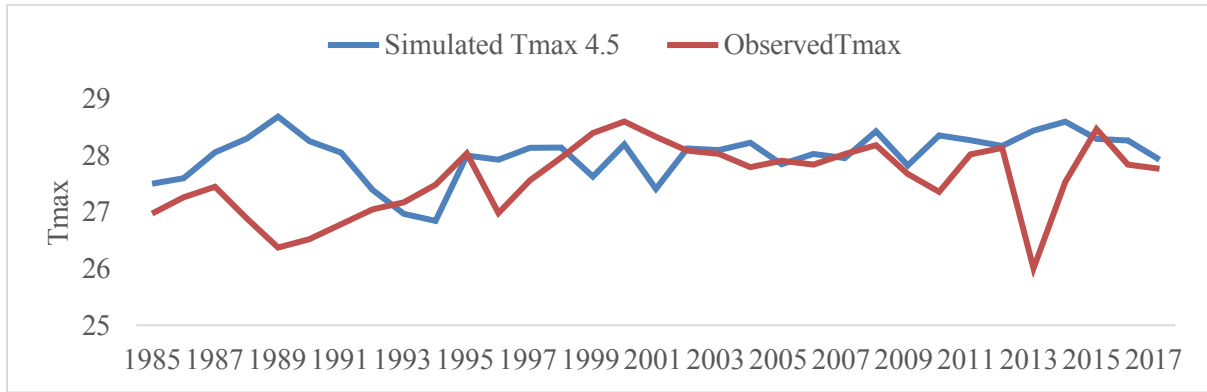


Figure 4. 7 Calibration result of average daily temperature simulated and measured at the near Jimma by 4.5 model.

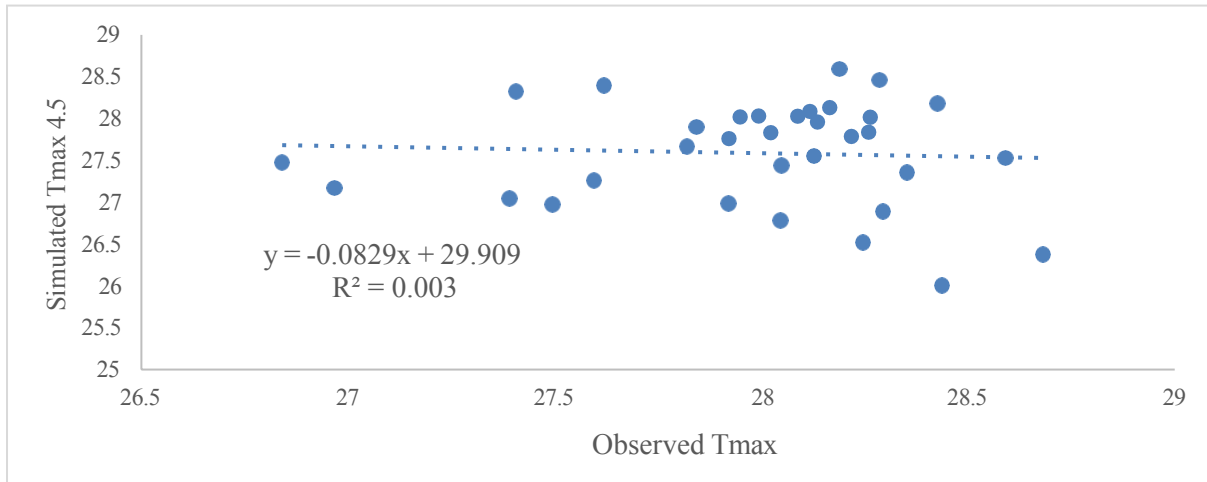


Figure 4. 8 Values of R^2 for calibration period

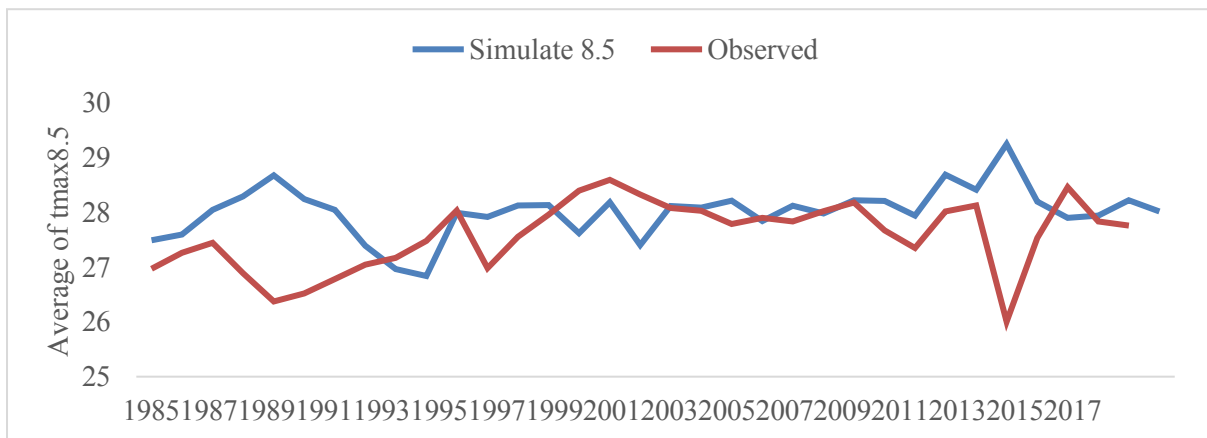


Figure 4. 9 Calibration result of average daily temperature simulated and measured at the near Jimma by 8.5 model.

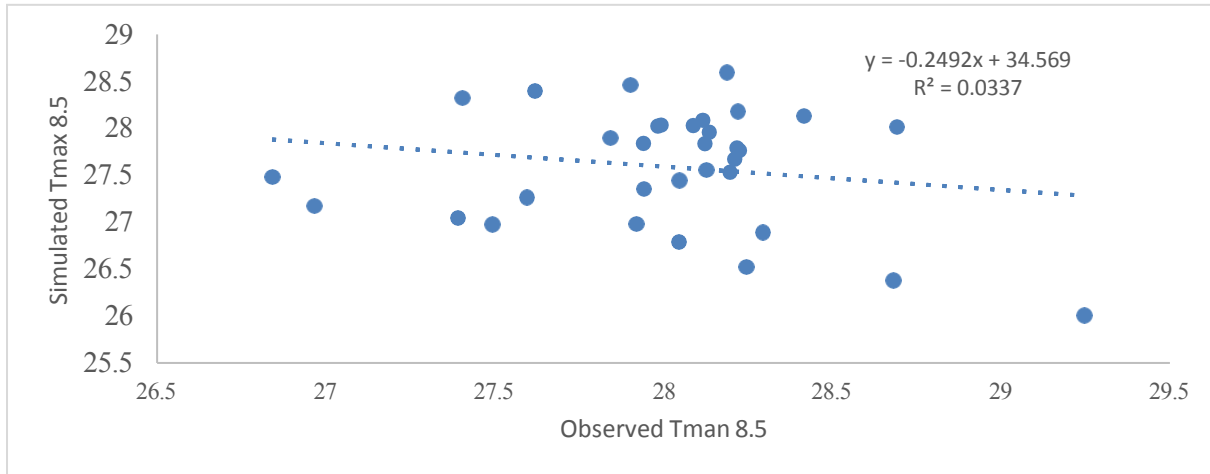


Figure 4. 10 Values of R^2 for calibration period

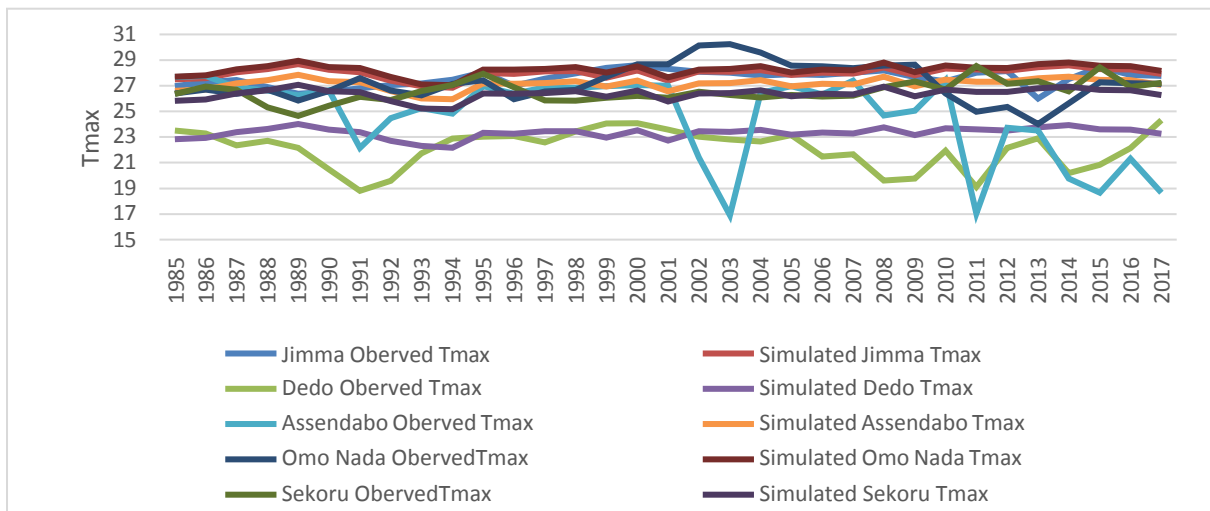


Figure 4. 11 Calibration result of average daily temperature simulated and measured at the all stations by 4.5 model.

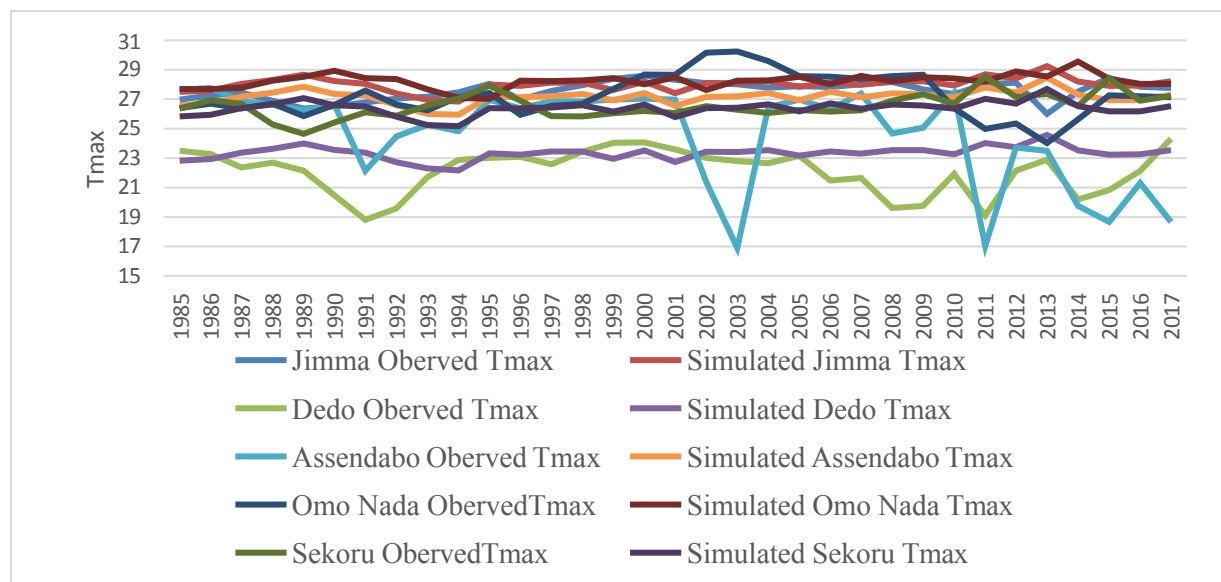


Figure 4. 12 Calibration result of average daily temperature simulated and measured at the all stations by 4.5 model.

Minimum Temperature Model Performance

Table 4.3, figure 4.14 and figure 4.15 shows the statistical indicators (minimum temperature) obtained for weather stations against the different satellite estimates. In general, the result shows a satisfactory agreement between the observed and simulated minimum temperature. In terms of bias all stations were performed satisfactorily except Assendabo (bias=20.236) and Dedo (bias=10.3153) which indicate fit and linear association between observed and simulated minimum temperature is unsatisfactory, where Sekoru (Bias=1.3494) shows good best performance. However, coefficient of correlation (r) is shows quite good There is a strong correlation (i.e. linear relationship) between the minimum temperature amount from most models and the reference data, the average magnitude of estimated error, RMSE, is quite larger in minimum observed and simulated temperature.

Figure 4.17 shows the scatter plots produced between the point-based Jimma data of the observed stations versus simulated minimum temperature. A relatively lower coefficient of determination values ($R^2 = 0.005$) was observed for Jimma Tmin estimates. The trend line of Jimma Tmin is converging to the 45° line, which shows the existence of a good agreement between Jimma observed and simulated minimum temperature.

Table 4. 3 Performance of the CORDEX-RCM simulations in capturing and representing mean annual maximum temperature over the upper Gilgel Gibe basin over the period 1985–2017.

Scenario Tmin	Performance Statistic	Stations				
		Jimma	Ascendabo	Dedo	Omonad	Sekoru
RCP4.5	Statistical analysis					
	RMSE	2.5512	4.3886	2.8151	2.527	2.5169
	PBIA	7.1488	20.2364	10.3153	6.939	1.3494
RCP8.5	r	-0.0718	0.5918	-0.0695	0.024	0.2494
	RMSE	2.5957	4.4108	2.8721	2.568	2.5432
	PBIA	7.3753	19.4281	10.5585	7.254	1.6420
	r	-0.1693	0.6397	-0.2123	-0.099	0.1518

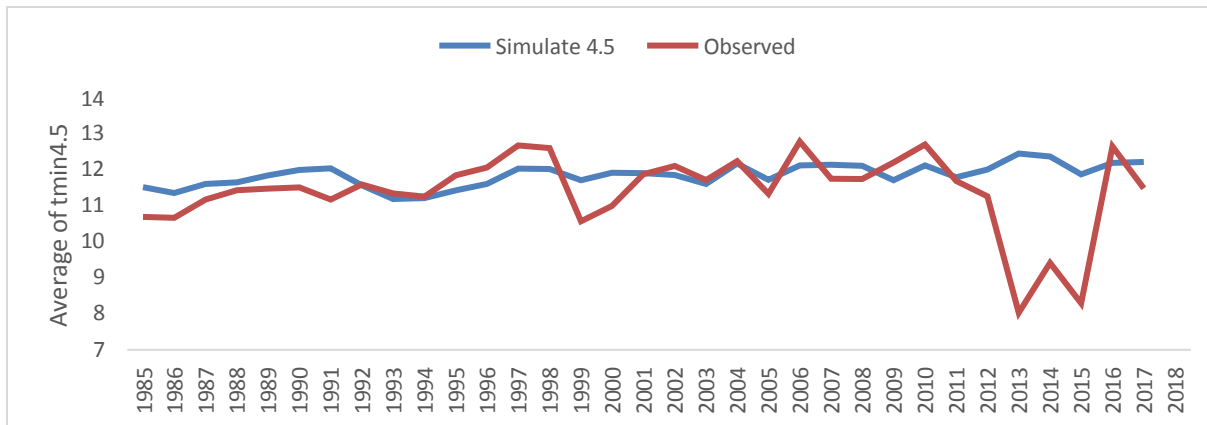


Figure 4. 13 Calibration result of average daily minimum temperature simulated and measured at the near Jimma by 4.5 model.

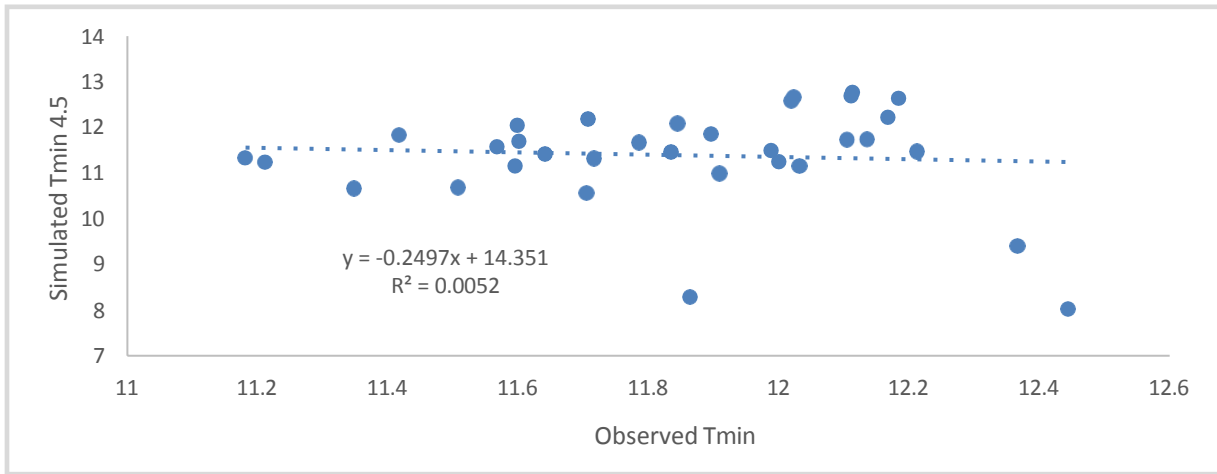


Figure 4. 14 Scatter diagram of computed and observed minimum temperature during calibration.

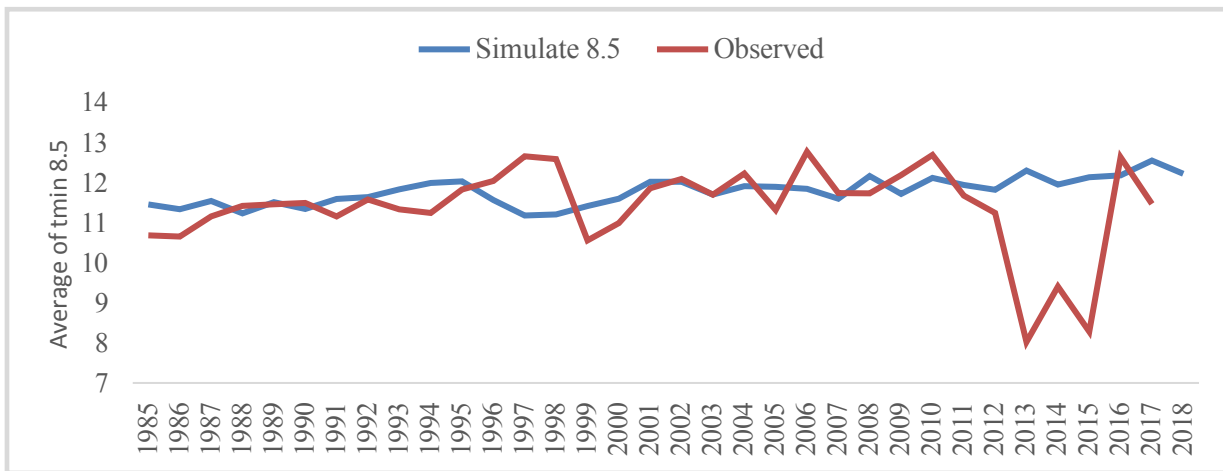


Figure 4. 15 Calibration result of average daily minimum temperature simulated and measured at the near Jimma by 4.5 model.

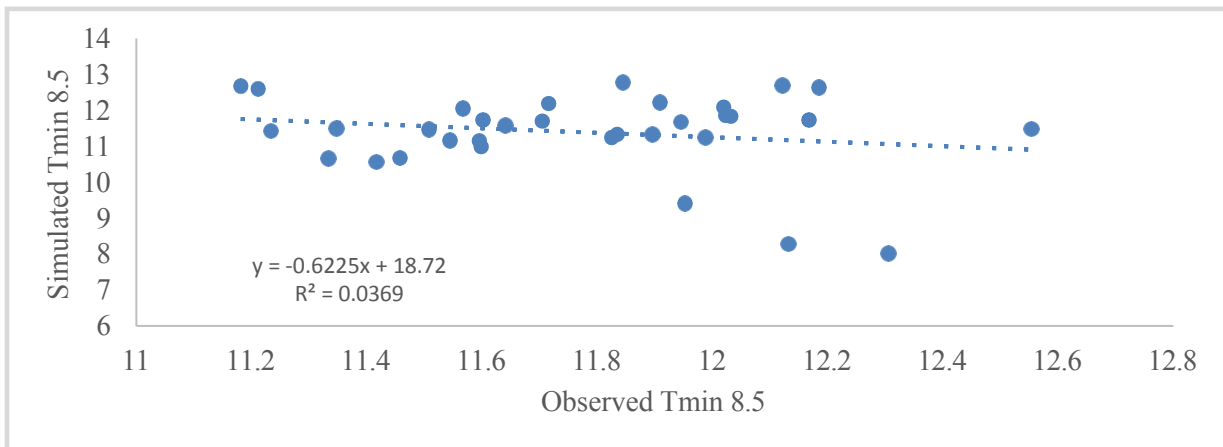


Figure 4. 16 Scatter diagram of computed and observed minimum temperature during calibration.

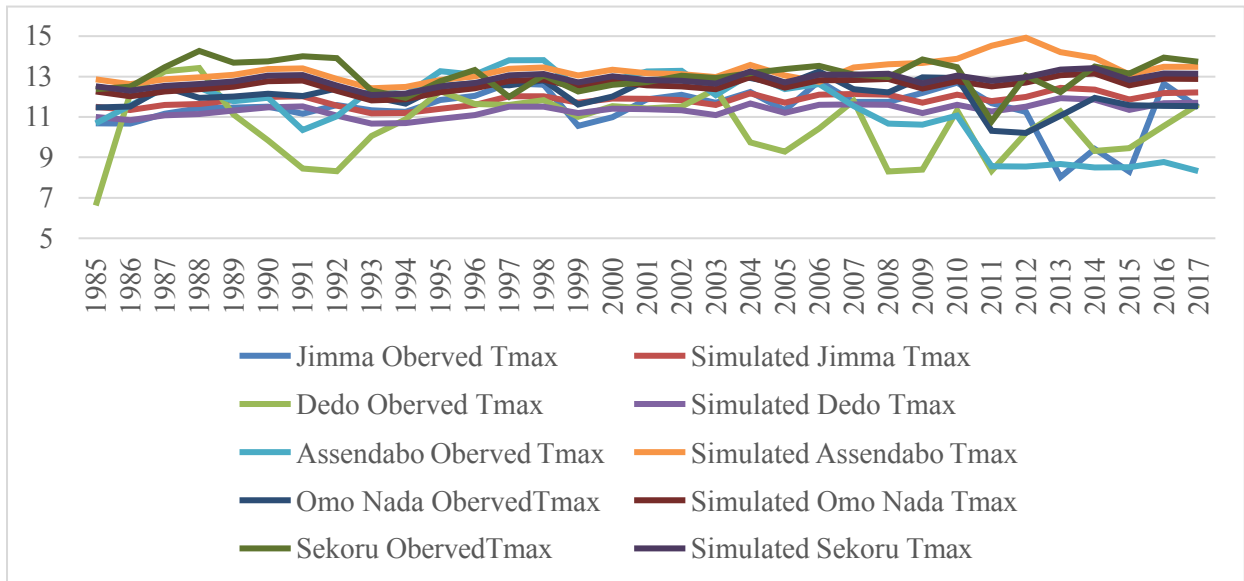


Figure 4. 17 Calibration result of average minimum temperature simulated and measured at the all stations by 4.5 model.

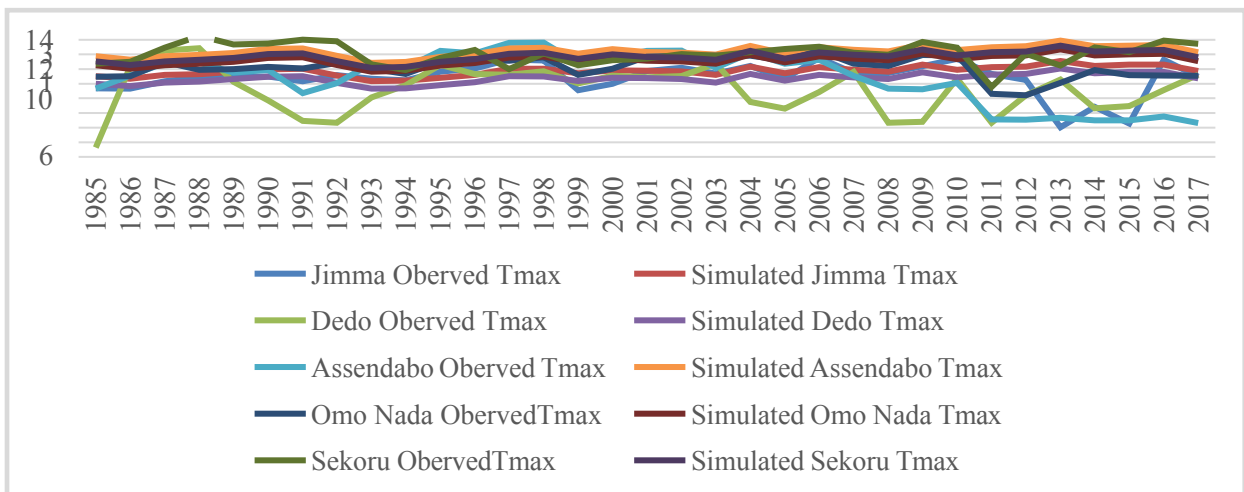


Figure 4. 18 Calibration result of average minimum temperature simulated and measured at the all stations by 8.5 model.

Descriptive statistics and variability analysis

The annual and seasonal mean of time series data of climatic parameters, particularly temperature (maximum and minimum) and precipitation were analyzed using MK for five sub-basins. In the MK test, parameters like P Value, S statistic, and the Z statistic were considered to identify the increasing or decreasing trend in the time series of climatic parameters. The test results were discussed below.

Rainfall

Table.4.1 shows basic statistics and MK trend analysis of rainfall in Jimma sub-basin. The mean annual rainfall of the area during the study period was 55.66cm with 9.85cm standard deviation and 18.03 CV. The minimum and maximum ever recorded rainfalls were 2.61 cm (in 2017- the driest year) and 6.45cm (in 1992-the wettest year) per year respectively. As depicted in Table 2, summer is the major rain season in the study area which contributes about 47.12 % of the total rainfall. The short rainy season which lasts from December to February (called winter (belg)) also contributes a substantial amount of rainfall (around 5.65% of the total).

Table 4. 4 Basic Statics and MK trend analysis of rainfall in Jimma sub-basin (1985-2018)

Month	Min	Max	Mean	%	SD	CV (%)	Z-MK test	P-value	Sen's Slope
Spring	8.88	21.42	15.15	27.72	3.36	22.16	-1.38	0.17	-0.17
Summer	9.14	45.55	25.75	47.12	6.71	26.05	-1.38	0.17	-0.17
Autumn	5.36	22.47	10.72	19.61	3.64	33.95	-0.64	0.53	-0.08
Winter	0.1	8.41	3.09	5.65	1.96	63.43	-0.67	0.51	-0.02
Annual	31.19	77.16	54.66	100	9.85	18.03	-0.39	0.7	-0.1

When the rainfall amount of the recent decades (1985–2017) is compared with the future decades (2025-2050), a dramatic reduction in annual mean and summer (main rainy season) was predicted. For instance, the mean annual, spring, summer, autumn and winter rainfall in the study area from 1985 to 2017 was 54.66cm, 15.15cm, 25.75cm, 10.72cm and 3.09cm respectively. This amount will be decreased to 49.84cm, 12.67cm, 23.95cm, 11.64cm and 1.58cm during 2025-2050, when there is no increasing of greenhouse gas emission for annual, spring, summer, autumn and winter respectively, and when there is increasing greenhouse gas this amount will decrease 52.21cm, 12.37cm, 26.54cm, 11.56cm, and 1.65 for annual, spring, summer, autumn and winter respectively. As depicted in Table 4.4, though the declining trend of winter rainfall is not statistically significant,

the CV (63.43) is higher than that of winter rainfall (26.05) which implies more interannual variability of winter(belg) rainfall than summer(kiremt) one.

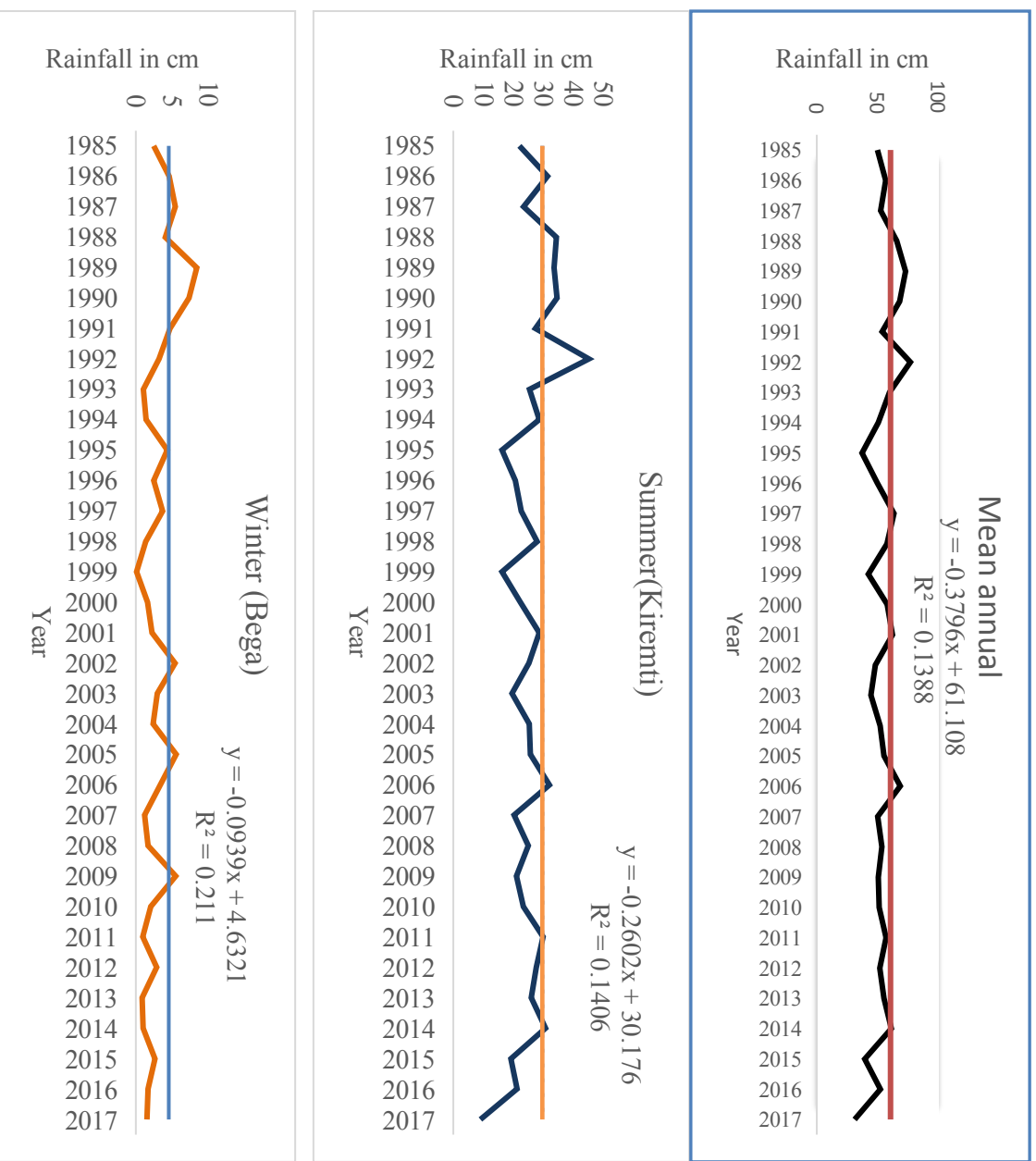


Figure 4. 19 Rainfall pattern of (Annual, kiremt and belg) Jimma sub-basin (1985–2017)

Using a linear regression model (Fig 4.1), the rate of change is defined by the slope of regression line which in this case is about -0.396cm/year, -0.262cm/year and -0.0939cm/year for annual, summer and winter rainfall respectively. The declining trend for summer rainfall in Jimma ($P < 0.05$) was found to be statistically significant negative trend while those of annual and winter was non-significant (Table 4.4). The rainfall anomaly also witnessed for the presence of inter-annual variability and the trend being below the long-term average becomes more pronounced particularly since the 1985.

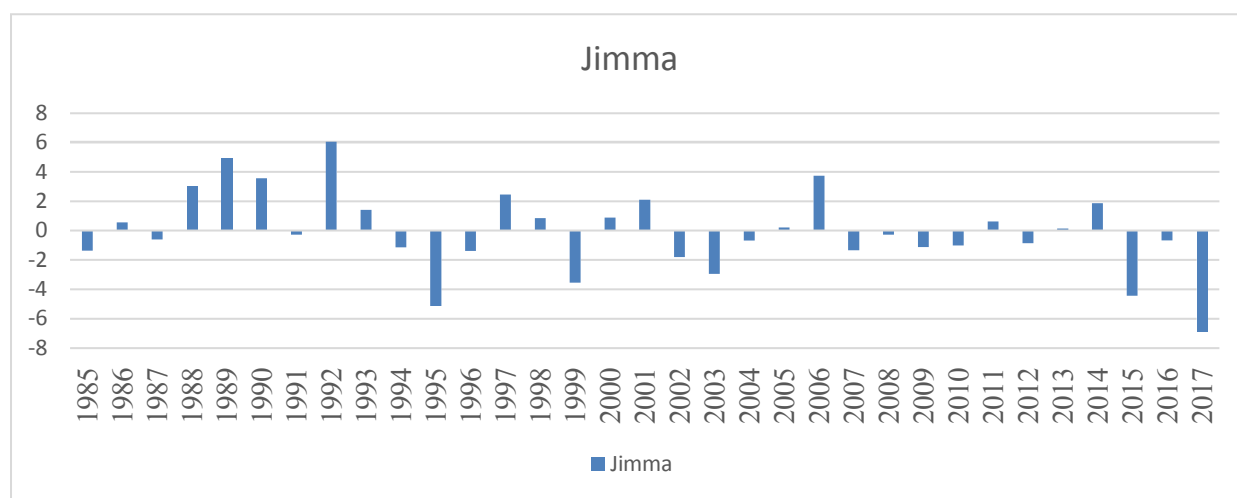
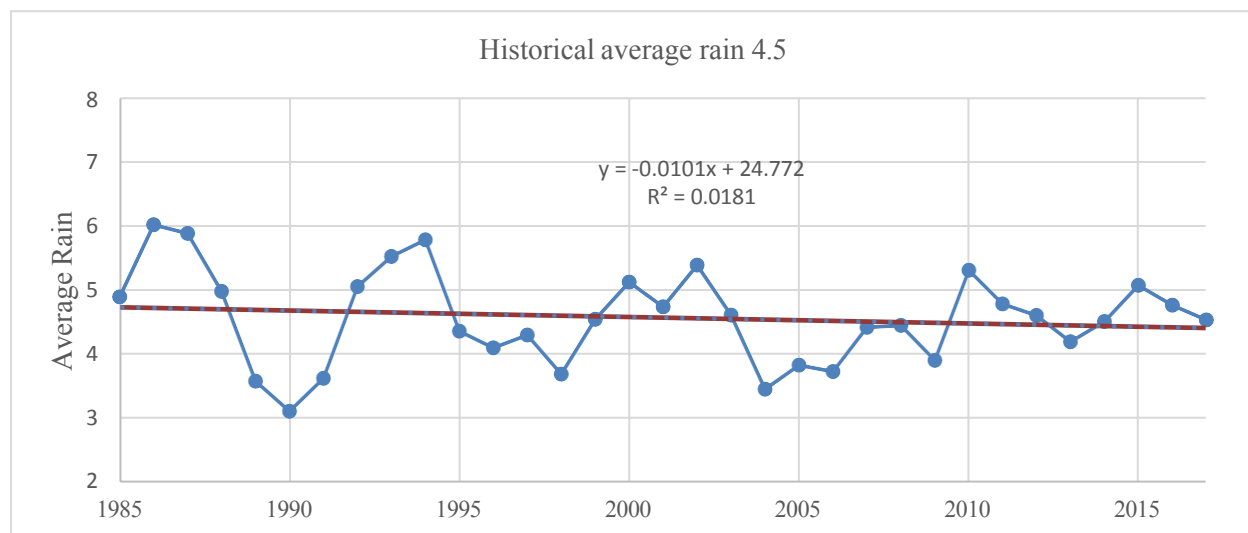


Figure 4. 20 Rainfall Anomalies of Jimma sub-basin (1985–2017)



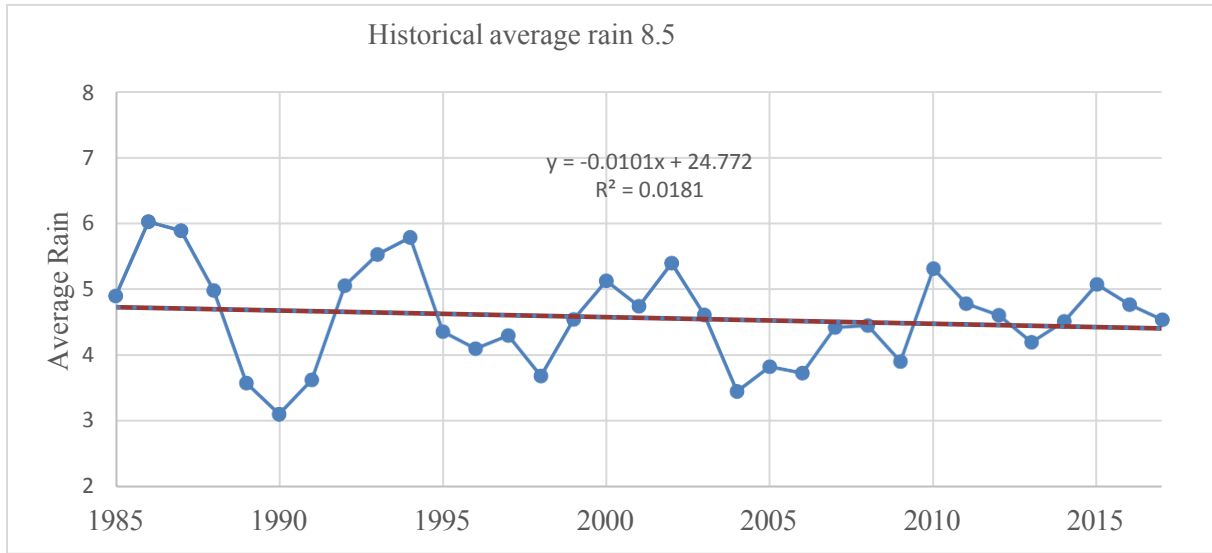


Figure 4. 21 Trends of mean annual precipitation for the Jimma Station in historical period under RCP4.5 & RCP8.5

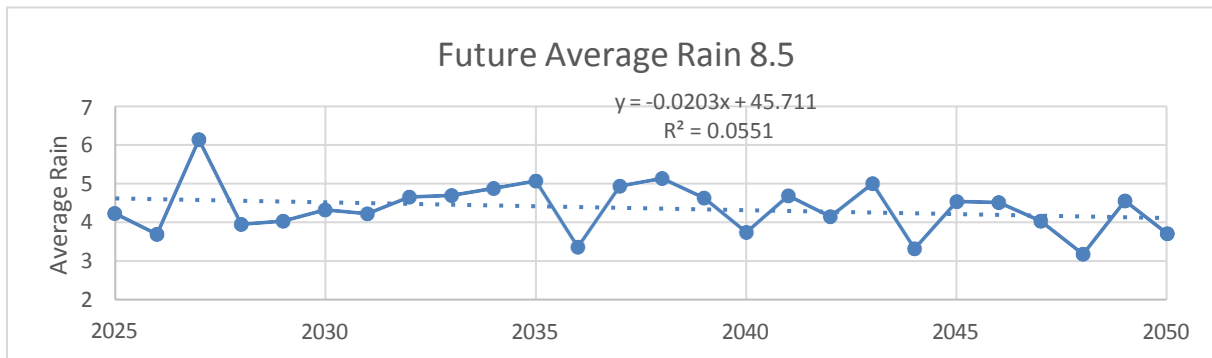
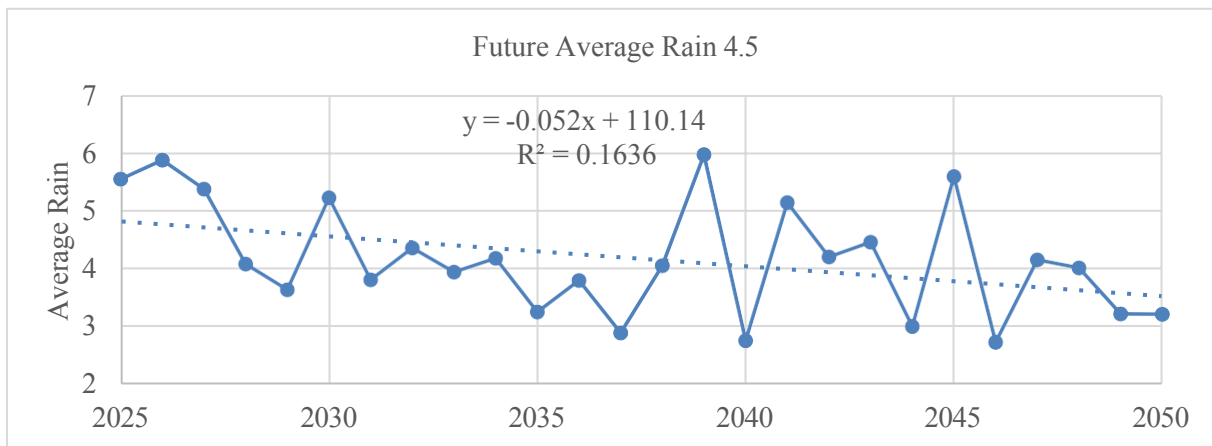


Figure 4. 22 Trends of annual precipitation for the Jimma station 2025-2050 period under RCP4.5 & RCP8.5.

The same as Jimma station was taken to analysis the basic statistics and MK trend of rainfall in Dedo, Assendabo, Sekoru, and Omonada. The table and figures of the result are shown in the Appendix, and short result and discussion of those stations are as follows:

For Dedo the mean annual rainfall of the area during the study period was 54.951cm with 13.330cm standard deviation and 24.26% of CV, with annual rate of change of -0.0101cm/year. The declining trend for annual rainfall in Dedo ($S=-26.00$, $P=0.70$) was found to be non-statistically significant negative trend.

For Assendabo the mean annual rainfall of the area during the study period was 47.13cm with 9.21cm standard deviation and 19.54% of CV, with annual rate of change of -0.00441cm/year. The declining trend for annual rainfall in Assendabo ($S=-34.00$, $P=0.61$) was found to be statistically non-significant negative trend.

For Sekoru the mean annual rainfall of the area during the study period was 43.21cm with 7.61cm standard deviation and 19.76% of CV, and annual rate of change of -0.00441cm/year. The declining trend for annual rainfall in Assendabo ($S=-24.00$, $P=0.72$) was found to be statistically non-significant negative trend.

For Omonad the mean annual rainfall of the area during the study period was 60.321cm with 9.62cm standard deviation and 16.07% of CV, and annual rate of change of -0.0057cm/year. The declining trend for annual rainfall in Assendabo ($S=-40.00$, $P=0.55$) was found to be statistically non-significant negative trend.

Temperature

An increase in temperature is among the manifestations of global climate change. Analysis of annual and seasonal temperature for Gilgel Gibe was undertaken to detect the variability and trend of temperature change in the study area under two scenarios (RCP4.5 and RCP8.5).

Table 4. 5 MK trend analysis of Tmax in Jimma sub-basin.

Mann-Kendall test historical Tmax (1985-2017)						
Temperature scenarios	Statistical Analysis	Spring	Summer	Autumn	Winter	Annual
RCP 4.5	Z-value	-0.36	2.84	1.26	1.32	2.15
	Sen slopes	-0.02	0.08	0.06	0.06	0.17
	S	-24.00	184.00	82.00	86.00	140.00
	P-Value	0.72	0.005	0.21	0.19	0.03
RCP 8.5	Z-value	0.45	2.34	1.26	1.26	1.84
	Sen slopes	0.04	0.06	0.06	0.07	0.14
	S	30.00	152.00	82.00	82.00	120.00
	P-Value	0.65	0.02	0.21	0.21	0.07
Mann-Kendall test Future Tmax (2025-2050)						
RCP 4.5	Z-value	0.62	0.00	1.28	-0.40	0.97
	Sen slopes	0.09	0.01	0.11	-0.08	0.40
	S	29.00	1.00	59.00	-19.00	45.00
	P-Value	0.54	1.00	0.20	0.69	0.33
RCP 8.5	Z-value	3.26	4.14	2.78	2.78	4.36
	Sen slopes	0.49	0.27	0.26	0.22	1.01
	S	149.00	189.00	127.00	127.00	199.00
	P-Value	0.0005	0.0001	0.01	0.01	0.0002

The above Mann-Kendall test result is shown that the basin has an increasing maximum temperature trend in summer, autumn, and annual (Sens slope is positive) but trends shows non-significant increasing in autumn and winter ($P=0.21$, $P=0.19$), where summer and annual were significant increasing ($P=0.005$, $P=0.03$) and spring maximum temperature shows non-significantly decreasing ($S=-24.00$, $p=0.72$) under historical low-medium concentration (1985-2017, RCP-4.5). Under historical high concentration scenario there is non-significant increasing of maximum temperature in spring, autumn, winter and annual, while there is significant increasing in summer ($S=152.00$, $P=0.02$).

Also, the result shows increasing of maximum temperature under both scenarios of high concentration and low medium concentration (RCP8.5 and RCP4.5, 2025-2050), the P-value estimate indicate non-significant increase under low-medium concentration (RCP4.5), and significant increase under high concentration (RCP8.5).

Table 4. 6 MK trend analysis of Tmin in Jimma sub-basin.

Mann-Kendall test historical Tmin (1985-2017)						
Temperature scenarios	Statistical Analysis	Spring	Summer	Autumn	Winter	Annual
RCP 4.5	Z-value	2.40	4.29	2.09	1.69	3.92
	Sen slopes	0.05	0.07	0.04	0.07	0.26
	S	156.00	278.00	136.00	110.00	254.00
	P-Value	0.02	0.0001	0.04	0.09	0.0001
RCP 8.5	Z-value	2.80	4.17	3.42	2.18	4.26
	Sen slopes	0.06	0.07	0.07	0.08	0.30
	S	182.00	270.00	222.00	142.00	276.00
	P-Value	0.01	0.0003	0.0006	0.03	0.0002
Mann-Kendall test Future Tmin (2025-2050)						
RCP 4.5	Z-value	2.03	3.35	1.15	1.76	3.31
	Sen slopes	0.08	0.08	0.03	0.10	0.32
	S	93.00	153.00	53.00	81.00	151.00
	P-Value	0.043	0.001	0.252	0.078	0.001
RCP 8.5	Z-value	3.92	4.98	1.41	0.35	3.75
	Sen slopes	0.18	0.13	0.04	0.02	0.44
	S	179.00	227.00	65.00	17.00	171.00
	P-Value	0.00002	0.00	0.16	0.72	0.0001

The above MK trend analysis shows that the basin has a significantly increasing minimum temperature in annually and all seasons, excluding winter, under both scenarios of high concentration and low-medium concentration (RCP8.5 and RCP4.5).

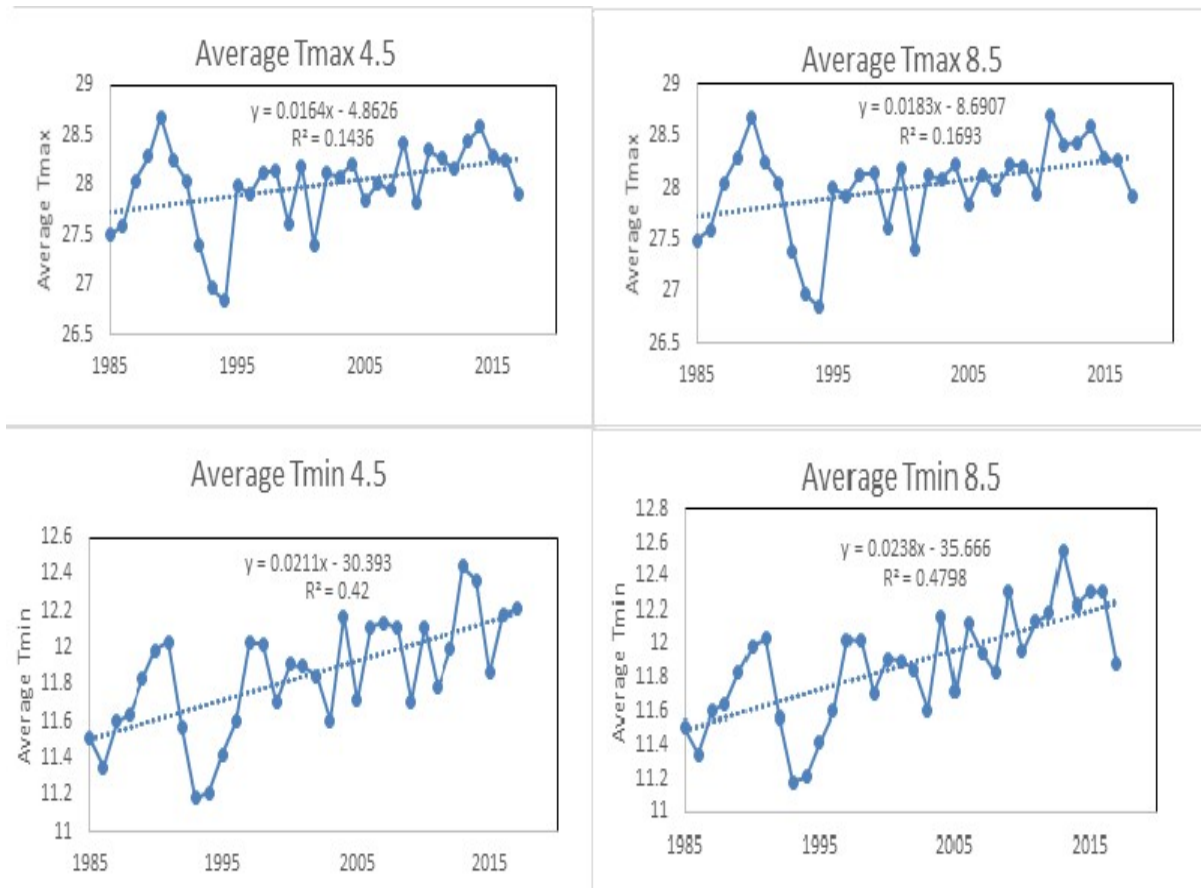


Figure 4. 23 Trends of maximum and minimum temperature plot in Jimma Station for historical

The mean temperature in the study area ranges from 11.84⁰ C (minimum) to 28.0⁰ C (maximum) with annual average temperature of 19.92⁰ C. Using a linear regression model, the rate of change is defined by the slope of the regression line (Figure 4.23) which in this case is about 0.0164⁰C and 0.0211⁰C per decade maximum and minimum temperature respectively under low-medium concentration (RCP4.5) during the period of 1985–2017, while there is rate of change of 0.0188⁰C and 0.0238⁰ C per decade of maximum and minimum temperature under high-concentration scenario (RCP8.5) with the same period.

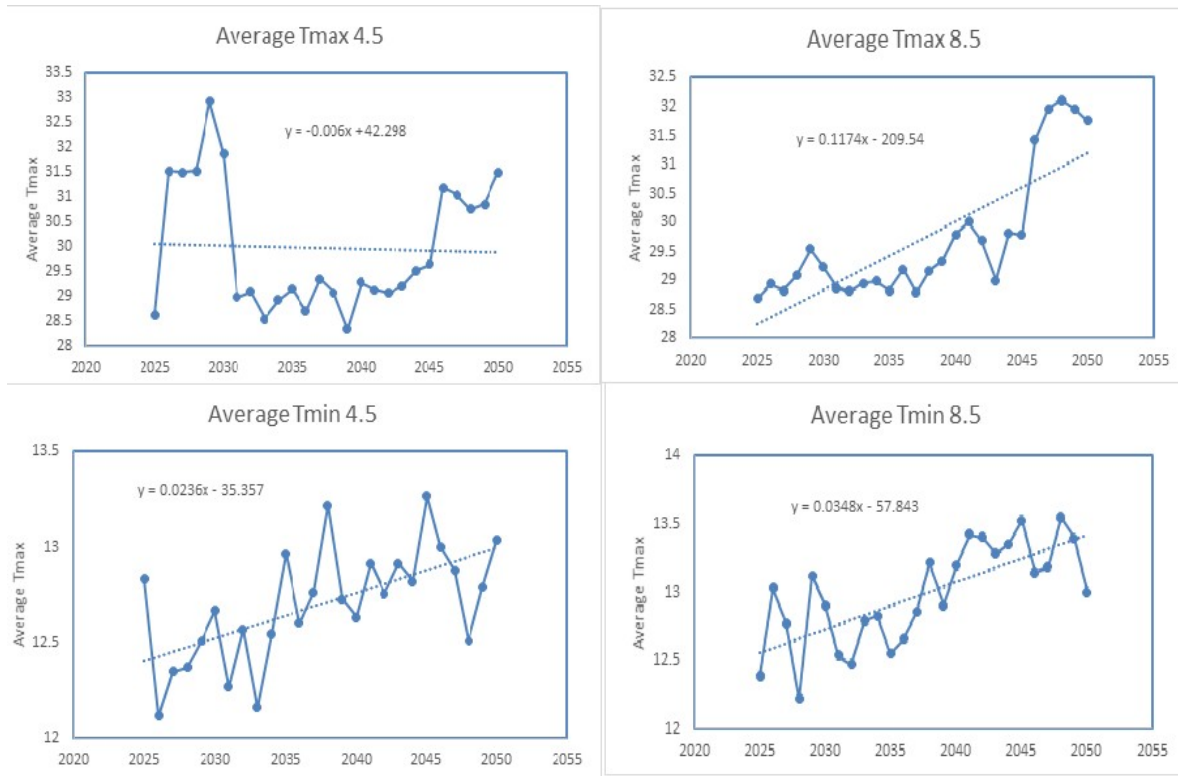


Figure 4. 24 Trends of maximum and minimum temperature plot in Jimma Station for future.

Figure 4.24 shows the mean temperature in the Jimma will ranges from 12.80°C (minimum) to 29.80°C (maximum) with annual average temperature of 21.34°C . Using a linear regression model, the rate of change is defined by the slope of the regression line (Figure 4.24) which in this case is about -0.006°C and 0.0236°C per decade maximum and minimum temperature respectively under low-medium concentration (RCP4.5) in the period of 2025-2050, while there is rate of change of 0.117°C and 0.0348°C per decade of maximum and minimum temperature under high-concentration scenario (RCP8.5) with the same period.

The same method as Jimma station was taken to analysis the basic statistics and MK trend of Maximum and minimum temperature in Dedo, Assendabo, Sekoru, and Omonada. The table and figures of the result are shown in the Appendix, and short result and discussion of those stations are as follows:

For Dedo Mann-Kendall test result is shown that the basin has a significant increasing maximum temperature ($S=140$, $P=0.03$), and minimum temperature ($S=254$, $P=0.001$) trend in annual with annual mean Tmax is 22.10°C , and Tmin is 10.59°C , and annual rate of change of $0.0164^{\circ}\text{C}/\text{year}$ under RCP 4.5 scenario.

For Assendabo Mann-Kendall test result is shown that the basin has a significant increasing maximum temperature ($S=130$, $P=0.047$), and minimum temperature ($S=264$, $P=0.0001$) trend in annually with annual mean Tmax is 25.42°C , and Tmin is 11.54°C , and annual rate change of $0.0164^{\circ}\text{C}/\text{year}$ under RCP 4.5 scenario.

For Sekoru Mann-Kendall test result is shown that the basin has a significant increasing maximum temperature ($S=130$, $P=0.0456$), and minimum temperature ($S=250$, $P=0.0012$) trend in annually with annual mean Tmax is 26.56°C , and Tmin is 13.06°C , and annual rate change of $0.0164^{\circ}\text{C}/\text{year}$ under RCP 4.5 scenario.

For Omonad Mann-Kendall test result is shown that the basin has a significant increasing maximum temperature ($S=130$, $P=0.0456$), and minimum temperature ($S=250$, $P=0.0012$) trend in annually with annual mean Tmax is 27.26°C , and Tmin is 12.13°C , and annual rate change of $0.0164^{\circ}\text{C}/\text{year}$ under RCP 4.5 scenario.

Future climate variables change

Change in precipitation

In order to investigate the changes in seasonal and mean annual areal rainfall of the basin the following attempt has been done based on rainfall events seasons in Ethiopian; such as: -Summer: which has the months of June, July and August this season is characterized by main rainy season, Autumn: September, October and November, Winter: December, January and February, and Spring small rainy season of March, April and May. The areal precipitation from observed and all projected precipitation in 1985-2017 to 2025 was averaged and compared with observed results. The anomalies of bias corrected mean annual of the Upper Gilgel Gibe river basin during the future periods of 2025-2050.

Table 4.7 and figure 4.25 indicate among all the stations, station Jimma projects the largest decrease in mean annual precipitation under RCP 8.5 scenario in the future period (~ -0.365) whereas Assendabo projects the smallest decrease in mean annual precipitation (~ -0.046) under RCP 4.5 scenario. At the other hand, the largest increase in mean annual precipitation was projected under Dedo ($\sim +0.065$) under RCP 4.5 scenario.

Table 4. 7 Anomalies of Mean annual rainfall on Upper Gibe basin during future period (2025-2050).

Station	Jimma		Ded0		Assendabo		Sekoru		Omonad	
	RCP4.5	RCP8.5	RCP4.5	RCP8.5	RCP4.5	RCP8.5	RCP4.5	RCP8.5	RCP4.5	RCP8.5
Mean Rainfall	-0.075	-0.36	0.065	0.05	-0.04	-0.08	0.017	0.04	-0.3	-0.34



Figure 4. 25 Anomalies of bias corrected mean seasonal precipitation in the future (2025-2050).

Figure Indicates the basin mean monthly rainfall will be decreasing in the summer (June-August) under two emission scenarios except for August under RCP4.5. Whereas the mean rainfall during the Spring (March-May) projection shows decreasing trend for RCP4.5 and RCP8.5 scenarios. The mean rainfall during the Autumn (September-November) projection shows increasing for the two emission scenarios except for November under RCP8.5 and RCP4.5 and during winter (December-February) projection shows non-significant trend.

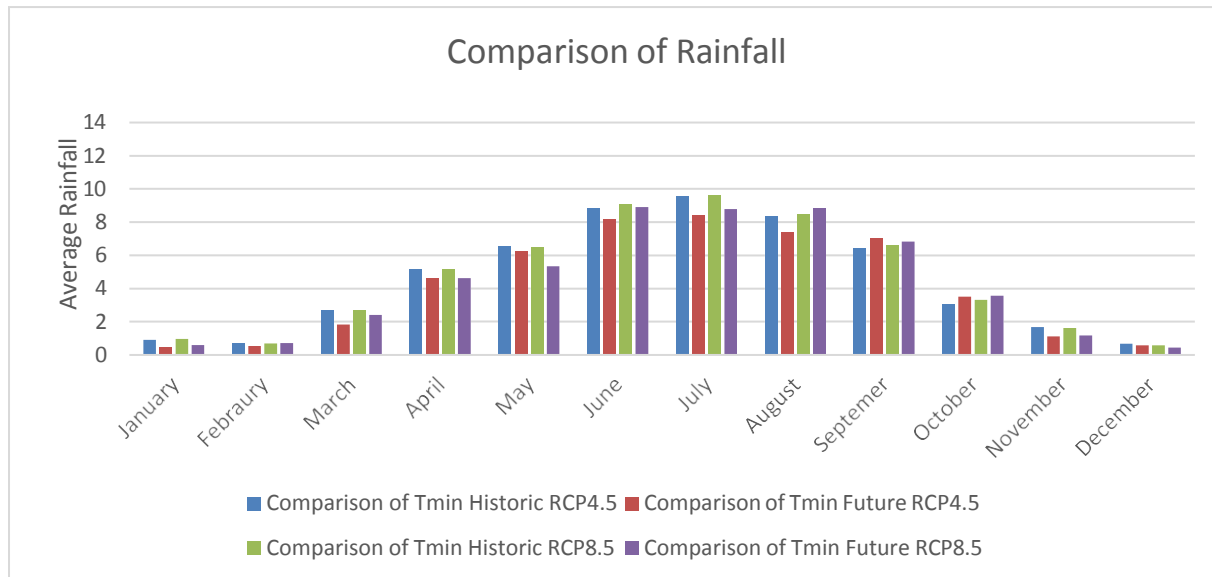


Figure 4. 26 Comparison of areal means monthly precipitation of historical (1985-2017) and future (2025-2050) with two scenarios RCP4.5 and RCP8.5 in Jimma station.

Change in temperature

Figure 4. shows the comparison of arithmetic average monthly maximum temperature in the catchment for temperature comparison in the study area. The RCP4.5 and RCP8.5 scenarios generation result showed that the maximum temperature increases in all months in the basin. Figure 4.8 shows that the comparison of arithmetic average monthly minimum temperature at upper Gilgel Gibe basin. It showed that the future minimum temperature increases in all months in the basin. Generally, the projected minimum and maximum temperature is within the range projected by IPCC, which reported average temperature rise by 1.4-5.80c towards the end of century (Adem et al, 2016). Maximum and Minimum temperature over equatorial east Africa will rise and that there will be warmer days compared to the baseline by the middle and end of century (IPCC, 2014).

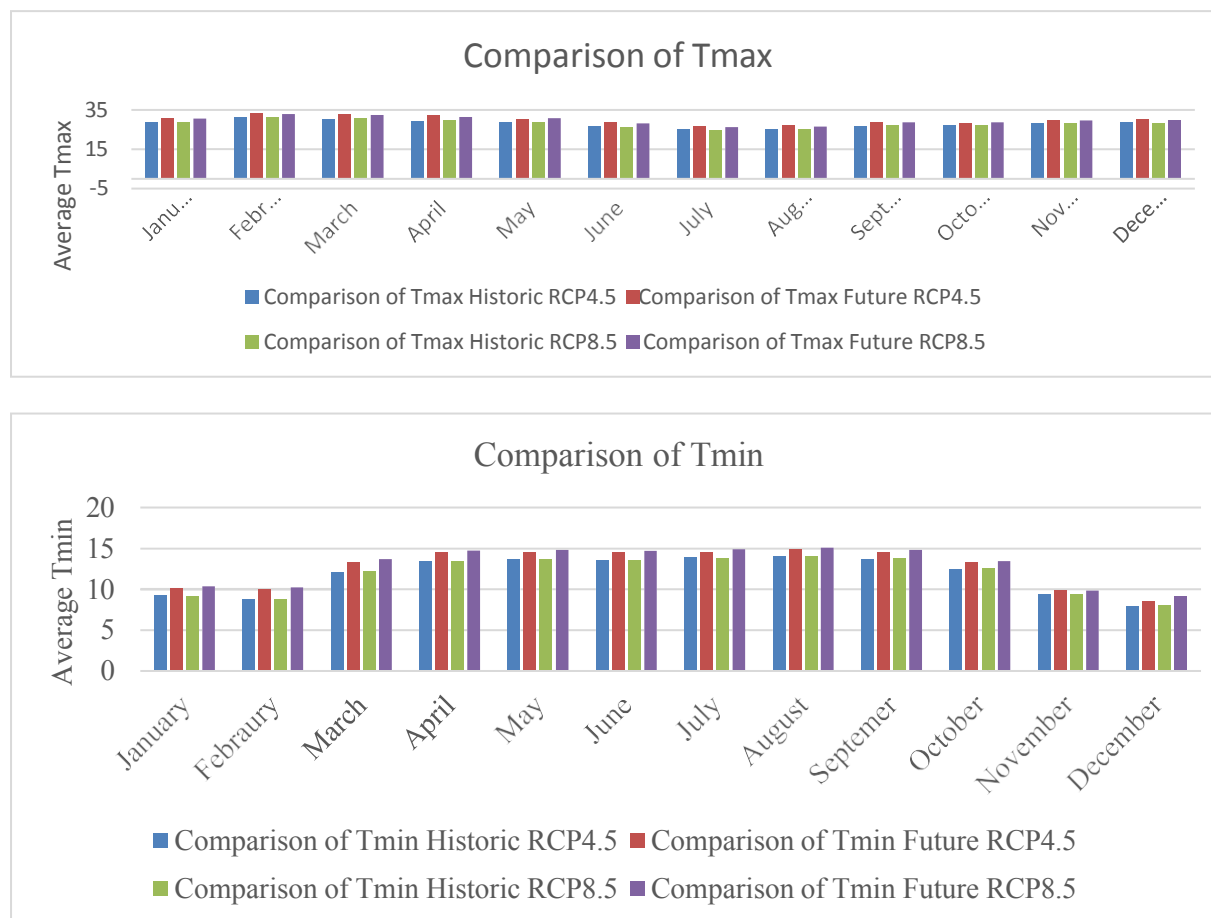


Figure 4. 27 Comparison of areal means monthly Minimum and maximum Temperature (1985-2017) and (2025-2050) with two scenarios RCP4.5 and RCP8.5 in Jimma station.

CONCLUSION AND RECOMMENDATION

Conclusion

This paper analyzed the long-term rainfall and temperature trend in Gilgel Gibe watershed. The trend analysis has been employed to inspect the change in rainfall and temperature in Gilgel Gibe watershed, using simulated precipitation and temperature data obtained for *CORDEX-RCM* and observed rainfall and temperature for five stations obtained from National Metrological Agent.

First the accuracy of simulation results was evaluated using a suite of statistical measures such as Bias, Root Mean Squared Error (RMSE) and correlation coefficient. Rainfall performance smallest bias (2.650, 3.810) was recorded Jimma station which shows its well captured and represented, where Sekoru shows high mean bias (10.416, 11.266) which shows that the data is satisfactorily captured and represented, under RCP4.5, and RCP8.5. For RMSE performance measure, Sekoru has the smallest value (112.4, and 119.3 mm per year under RCP4.5, and RCP8.5 respectively) whereas Dedo resulted in the largest value (162.4, 166.4mm per year under RCP4.5, and RCP8.5 respectively). In terms of bias, and RMSE, all stations were performed satisfactorily except Sekoru which performed poorest. However, when the correlation coefficient is used as an assessment criterion, there is a weak correlation between the annual rainfall amount from most models and the reference data. In maximum and minimum temperature result shows that there is satisfactory agreement in simulated and observed data.

Mann-Kendell test was used to detect the time series trend. The result revealed that there was non-significantly declining of trend for annual rainfall in all stations with rate change of: -0.0101cm/year, :0.0044cm/year: -0.00441cm/year, 0.0057cm/year, and -0.0939cm/year for Dedo, Assendabo, Sekoru, Omonad and Jimma, in 1985-2017 under RCP 4.5. When the rainfall amount of the recent decades (1985–2017) is compared with the future decades (2025-2050), a dramatic reduction in annual mean and summer (main rainy season) was predicted. Also, the rainfall anomaly also witnessed for the presence of inter-annual variability and the trend being below the long-term average becomes more pronounced particularly since the 1985. And for maximum and minimum temperature the result has shown that there is significant increasing in annually. The mean temperature in the study area ranges from 11.84⁰ C (minimum) to 28.0⁰ C (maximum) with annual average temperature of 19.92⁰ C, and the rate of change was 0.0164⁰C and 0.0211⁰C per

decade maximum and minimum temperature respectively under low-medium concentration (RCP4.5) during the period of 1985–2017, while there is rate of change of 0.0188°C and 0.0238°C per decade of maximum and minimum temperature under high-concentration scenario (RCP8.5) with the same period.

For general comparison basin rainfall, and temperature was calculated as arithmetic average value all station. The statistical indicated that the rainfall may decreasing of monthly of rainfall in 2025-2050 under RCP4.5 and RCP8.5 respectively. Average maximum temperature may warm and the minimum temperature will be increased.

REFERENCES

- Asfaw, A., Simane, B., Hassen, A., & Bantider, A. (2018). Variability and time series trend analysis of rainfall and temperature in northcentral Ethiopia: A case study in Woleka sub-basin. *Weather and Climate Extremes*, 19. <https://doi.org/10.1016/j.wace.2017.12.002>
- Dereje Ayalew. (2012). Variability of rainfall and its current trend in Amhara region, Ethiopia. *AFRICAN JOURNAL OF AGRICULTURAL RESEARCH*, 7(10). <https://doi.org/10.5897/ajar11.698>
- Jain, S. K., Kumar, V., & Saharia, M. (2013). Analysis of rainfall and temperature trends in northeast India. *International Journal of Climatology*, 33(4). <https://doi.org/10.1002/joc.3483>
- Jillo, A. Y., Demissie, S. S., Viglione, A., Asfaw, D. H., & Sivapalan, M. (2017). Characterization of regional variability of seasonal water balance within Omo-Ghibe River Basin, Ethiopia. *Hydrological Sciences Journal*, 62(8). <https://doi.org/10.1080/02626667.2017.1313419>
- Langat, P. K., Kumar, L., & Koech, R. (2017). Temporal variability and trends of rainfall and streamflow in Tana River Basin, Kenya. *Sustainability (Switzerland)*, 9(11). <https://doi.org/10.3390/su9111963>
- Mahajan, D. R., & Dodamani, B. M. (2015). Trend Analysis of Drought Events Over Upper Krishna Basin in Maharashtra. *Aquatic Procedia*, 4. <https://doi.org/10.1016/j.aqpro.2015.02.163>
- Mondal, A., Kundu, S., & Mukhopadhyay, A. (2012). Case Study 70 RAINFALL TREND ANALYSIS BY MANN-KENDALL TEST: A CASE STUDY OF NORTH-EASTERN PART OF CUTTACK DISTRICT, ORISSA. In *Online) An Online International Journal Available at (Vol. 2, Issue 1)*.
- Sen, P. K. (1968). Estimates of the Regression Coefficient Based on Kendall's Tau. *Journal of the American Statistical Association*, 63(324). <https://doi.org/10.1080/01621459.1968.10480934>
- Taxak, A. K., Murumkar, A. R., & Arya, D. S. (2014). Long term spatial and temporal rainfall trends and homogeneity analysis in Wainganga basin, Central India. *Weather and Climate Extremes*, 4. <https://doi.org/10.1016/j.wace.2014.04.005>
- Wagesho, N., Goel, N. K., & Jain, M. K. (2013). Temporal and spatial variability of annual and seasonal rainfall over Ethiopia. *Hydrological Sciences Journal*, 58(2). <https://doi.org/10.1080/02626667.2012.754543>